FCTUC DEPARTAMENTO DE ENGENHARIA CIVIL
FACULDADE DE CIÊNCIAS E TECNOLOGIA
UNIVERSIDADE DE COIMBRA

Optimization of the energy efficiency of lightweight steel buildings

Dissertação apresentada para a obtenção do grau de Mestre em Engenharia Civil na Especialidade de Mecânica Estrutural

Autor
Ana Gabriela Loureiro dos Santos

Orientadores
Helena Maria dos Santos Gervásio
Luís Alberto Proença Simões da Silva

Coimbra, Julho, 2016

RESUMO

Decisores políticos têm sido motivados por preocupações financeiras e ambientais para desenvolver estratégias e criar legislação de modo a diminuir o consumo energético. A Diretiva 2012/27/EU estabelece um quadro comum de medidas para a promoção de eficiência energética na União Europeia com vista a alcançar-se a meta de uma redução de 20% do consumo de energia primária até 2020.

De acordo com a UNEP 2007, o setor da construção é responsável por 36% dos gastos totais anuais de energia na União Europeia. Estima-se que a maior percentagem de energia gasta durante a fase operacional do edifício seja usada em sistemas HVAC e de iluminação. De tal forma que se torna essencial contribuir para o aumento da eficiência energética de edifícios ainda durante a fase de projeto, com a criação de produtos com baixas necessidades energéticas Este cenário diminuirá a dependência de sistemas mecânicos sem prejudicar a funcionalidade do edifício.

O objetivo desta pesquisa é a realização de uma análise de otimização da eficiência energética de um edifício residencial durante a sua fase operacional, focando-se em 'light steel framing' como sistema estrutural. O problema foi definido, começando-se por estabelecer todas as variáveis que teriam capacidade para influenciar a eficiência energética do edifício, variáveis estas apenas relacionadas com a fase de projeto de engenharia civil. Dessa forma, sistemas de HVAC e de iluminação artificial estariam completamente excluídos como variáveis do estudo, por não pertencerem ao domínio. Adicionalmente, o efeito da alteração de parâmetros (tamanho da população e número de gerações) foi estudado de modo a atingir-se a solução ótima. Finalmente, foi analisada a influência de condições atmosféricas regionais, através da realização de análises de otimização para o mesmo modelo em diferentes zonas climáticas. Nas simulações foi utilizado o software DesignBuilder, versão 4.6.0.015.

Concluiu-se neste estudo que a qualidade do 'Pareto set' se encontra diretamente relacionada com a escolha dos parâmetros de simulação. Com uma população inicial de 5 elementos e 250 gerações são obtidos resultados superiores para este problema, traduzindo-se numa significativa redução do consumo energético. Apesar do aumento nos custos de capital, foi provado que a redução dos custos operacionais beneficiará o dono do imóvel a curto prazo. Os níveis de conforto do edifício foram incrementados, mostrando-se que é possível reduzir a dependência energética sem comprometer a funcionalidade do edifício.

ABSTRACT

Energy policy makers have been prompted by financial and environmental concerns to develop strategies and create legislation in order to reduce energy consumption. The Directive 2012/27/EU on energy efficiency establishes a common framework of measures for the promotion of energy efficiency within the European Union in order to achieve the target of 20% reduction in primary energy consumption for the year 2020.

According to the UNEP 2007, the construction sector is accountable for 36% of the overall yearly spending of energy in the European Union. It is estimated that the largest percentage of the energy used during the operational stage for space conditioning is spent by HVAC and lighting systems. Thus, it is essential to increase the energy efficiency of residential buildings already during the project phase, to create products with low energy needs right from the beginning. This scenario will diminish the dependency on mechanical systems to keep a building functional to its residents.

The aim of this academic research is to process an optimization analysis of the energy efficiency of a residential building during the operational stage, with light steel framing as a structural system. The problem was set up, starting by establishing all the variables that influence the energy efficiency of the building, exclusively related to the civil engineering project phase. In that way, HVAC and artificial lighting systems were completely excluded from the study as a variable, since they did not fit the domain. Additionally, the effect of changing simulation parameters (population size and number of generations) was studied to achieve superior optimal solutions. Finally, the influence of regional weather conditions was studied by conducting the optimization analysis for the same model in different climate zones. The software used for the simulations was the 4.6.0.015 version of DesignBuilder.

Based on this study, it is possible to conclude that the quality of the Pareto set is directly related to the choice of simulation parameters. The combination of a population size of 5 and 250 generations provides superior results for this problem, such as a significant decrease of total site energy consumption. Despite the increase of initial capital costs, it was proven that the decrease of operational costs would benefit the home owner in the long run. The comfort levels of the building were also improved separately, showing that is it possible for energy dependency to be reduced without compromising the functionality of the building.

TABLE OF CONTENTS

SYMBOLS

ac/h – Air changes per hour
cm – Centimeter
h – Hour
k – Number of objectives
kg – Quilogram
kWh – Kilowatt hour
m^2 – Square meter
mm – Milimeter
J - Joule
R – Measure of thermal resistance used in the building and construction industry (R-value)
s.t. – Such that
U – Overall heat transfer coefficient that describes how well a building element conducts heat or the rate of transfer of heat (in watts) through one square metre of a structure divided by the difference in temperature across the structure (U-value)
x – Feasible solution
X – Feasible set of decision vectors
^{0} C – Degree Celsius
^{o} F – Degree Fahrenheit
$\in$ - Element of

ABBREVIATONS

ABUPS – Annual Building Utility Performance Summary
AC – Air Conditioning
ADENE **–** Agência para a Energia
ASHRAE – American Society of Heating, Refrigerating and Air Conditioning Engineers
CDH – Cooling Degree Hours
CE - Certificado Energético e da Qualidade do Ar Interior
COP – Coefficient of Performance
DCR - Declaração de Conformidade Regulamentar
EC – European Community
ECV – Energy Consumption Variation
EU – European Union
EU-25 – European Union constituted by the member states after the 2004 enlargement
GA – Genetic Algorithm
HDH – Heating Degree Hours
HVAC – Heating, Ventilation and Air Conditioning
LSF – Light Steel Framing
OT – Operative Temperature
OTV – Operative Temperature Variation
PSA – Particle Swarm Algorithm
PVC – Polyvinyl Chloride
RCCTE – Regulamento das Características de Comportamento Térmico dos Edifícios
SCE – Sistema Nacional de Certificação Energética e da Qualidade do Ar Interior nos Edifícios
SHGC – Solar heat gain coefficient
TN – Tennessee
UNEP – United Nations Environment Programme
UPVC – Unplasticized Polyvinyl Chloride
US – United States
USC – University of Southern California

1 INTRODUCTION

1.1 Framework of the study

Throughout the twentieth century, there was a steep increase of housing unit size and numbers due to developments of the construction process, ease of access to housing credit and general economic growth. Additionally, more equipment and home appliances that need electrical energy to function have been made available to the public; such as computers, microwaves, entertainment systems and HVAC. These three factors combined culminated in an escalation of the levels of energy consumption in residential houses. In the EU, the construction sector is responsible for an estimated 36% of the total energy consumption (UNEP, 2007). The existing EU-25 building stock is compromised of single-family houses (53%), multi-family houses (37%) and high-rise buildings (10%) and a general trend of higher energy demand has been registered in single-family houses (Nemry et al, 2008). According to "Energy Efficiency and Renewable Energy" (2008) by the US Department of Energy, residential energy consumption has increased overall by about 34 percent from 1985 to 2004.

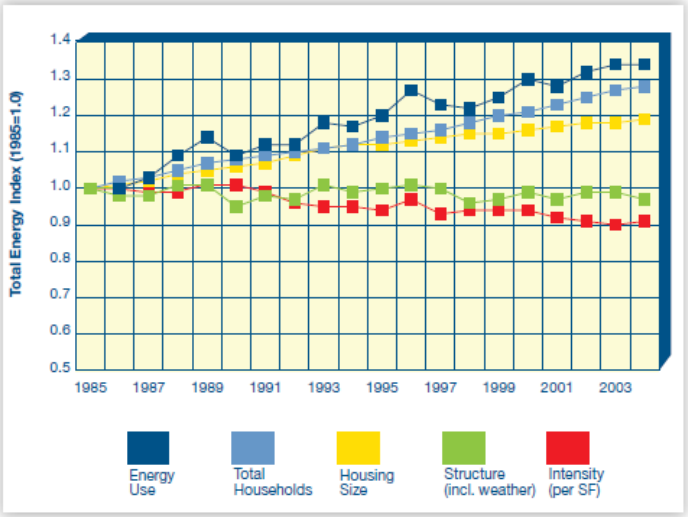

Figure 1.1 – Energy Use Intensity and Factors in the Residential Sector (US Department of Energy, 2008)

At the same period of time, annual energy consumption levels increased from 1,78 x 10^{17} J to 1,88 x 10^{17} J for a single model household (US Department of Energy, 2008). The expansion of the residential space is responsible for boosting even more the biggest portion of the energy use, which goes directly towards space conditioning (54%), in the form of space heating

(30,2%), space cooling (12,3%) and lighting (11%). The breakdown of the primary energy is illustrated in Figure 1.2.

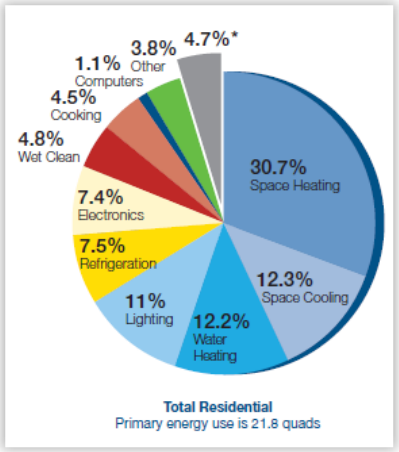

* The chart includes one quad of energy (4.7%) that constitutes a statistical adjustment by the US Energy Information Administration to reconcile two divergent data sources.

Figure 1.2 – Residential Primary Energy End-Use Splits, 2005 (US Department of Energy, 2008)

The most prominent sources of energy for buildings are electricity, natural gas and petroleum, in descending order. The purchase of energy has been rising to account for the growing demand, exemplified by an increase of 39,5% of the expenses with electricity from 1980 to 2005 (US Department of Energy, 2008). Buildings account for approximately 72% of the electricity and 36% of the natural gas consumption in the United States territory, with residential energy consumption being the most significant share in 2005.

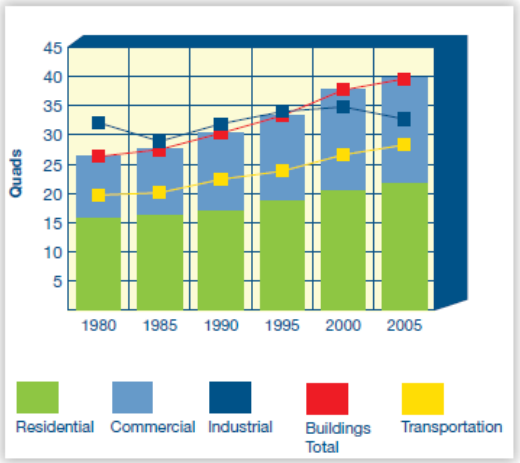

Figure 1.3 – Growth in Buildings Energy Use Relative to Other Sectors (US Department of Energy, 2008)

The reliance on electricity to cover the energy needs causes buildings to become the number one cause for the largest share of US carbon dioxide emissions, which has risen from 33% in 1980 to 40% in 2005 (US Department of Energy, 2008). The production of electricity is still mostly done with fossil fuels, like oil, coal and natural gas; despite the latest efforts of replacing these sources with renewable energy. Carbon dioxide emissions originate severe environmental and public health impacts, like global warming, air pollution and respiratory illnesses. Studies have demonstrated that is possible to reduce the emissions of greenhouse gases from European buildings by around 30% to 50% over the next 40 years, through the application of low-energy standards (Nemry et al, 2008).

As stated by Mardookhy (2013), HVAC and lighting systems account for 52-72% of the average energy consumed to perform space conditioning in a residential building. Therefore, elimination of avoidable energy deficits and increasing natural storage of energy through self-sufficient building presents itself as the solution regarding overdependence on external systems. This hypothesis will be explored as the central theme of this work.

1.2 General research objectives

This thesis focuses on the validation of the concept that seeking self-sufficiency of the building right from the initial stage of building design will result in a significant reduction of dependency from mechanical systems to achieve a good energy performance.

Therefore, the main goals of this thesis are:

i) To provide general guidelines about the calibration and optimization procedure;
ii) To identify the most influencing factors in the thermal performance of lightweight steel buildings, targeting residential houses;
iii) To achieve improvements in the performance of the building after undergoing the optimization process, leading to the minimization of the energy needs for cooling and heating and operational CO2 emissions;
iv) To test the premise that enhancing the energy performance of the building can be compatible with maintaining or even improving the comfort levels of the living space for its users, without worsening them;
v) To assess the fluctuations of performance of the building with different climatic requirements, by extending the analysis to three climate zones;
vi) To evaluate the proposition that reducing the operational energy costs will outweigh the initial increase of the capital costs and will make financial sense for the home owner in the short/medium term.

1.3 Thesis structure

This thesis is divided into seven different chapters. Each chapter has a clear purpose, as described in the following paragraphs:

Chapter I: This chapter includes the contextualization of the global energy problem of buildings that provides the groundwork for this study to take place, the presentation of the objectives the work is aiming to achieve and the organization of the thesis.

Chapter II: This chapter includes a summary of the legislation regarding energy efficiency in the European Union and a brief description of the energy performance certification procedure.

Chapter III: Overview on the state of the art to highlight the evolution of the use of Genetic Algorithms (GAs) in civil engineering, particularly energy efficiency problems.

Chapter IV: Introduction to the optimization theory to present fundamental concepts to enable the understanding of the problem, such as the algorithm used by DesignBuilder's optimization tool, interpretation of the expected solutions and simulation parameters that influence the type and quality of the set of solutions.

Chapter V: Application of the optimization procedure to a case study, including a brief characterization of lightweight steel buildings regarding energy performance, general description of the model, analysis of the reference models, breakdown of all the variables that influence the energy performance of a building, a parametric analysis and optimization settings.

Chapter VI: Presentation of the optimization results of the case study and comparative analysis of the results obtained for the different climatic regions.

Chapter VII: Conclusion and discussion of the impact of the research.

2 REGULATIONS ON ENERGY EFFICIENCY IN THE EUROPEAN UNION

2.1 Legislation

In recent years, the European Union (EU) has provided legislation with the purpose of regulating the energy consumption of buildings, as a way to increase their energy performance. Clear goals have been also established in terms of minimizing energy consumption across the Member States. The 2010 Energy Performance of Buildings Directive (2010/31/EU) and 2012 Energy Efficiency Directive (2012/27/EU) are the main pieces of legislation.

The 2010/31/EU Directive was an amendment and expansion of the 2002/91/EC Directive on the energy performance of buildings, which first laid down the implementation of an energy certification system.

Under the 2002 Energy Performance of Buildings Directive the following requirements were established:

- The energy performance certificate should include reference values, such as the reference legal figures and benchmarks, so the consumers can make an informed decision regarding the building;
- The energy performance certificate should provide recommendations regarding the improvement of the energy performance of the building;
- Buildings occupied by public authorities and buildings frequently visited by the public should display their energy performance certificates in a clearly visible place for public consultation;
- The validity of the energy performance certificate should not exceed ten years.

Under the 2010 Energy Performance of Buildings Directive it was established the following:

- Energy performance certificates are to be included in all advertisements for the sale or rental of buildings to inform potential buyer/tenant of a building of its energy performance levels;
- EU countries must establish inspection schemes;

- All new buildings must be zero energy buildings by 31 December 2020 and public buildings by 31 December 2018;
- EU countries must set minimum energy performance requirements for new buildings, for the major renovation of buildings and for the replacement or retrofit of building elements;
- EU countries have to create lists of national financial measures and incentives to enhance the energy efficiency of their buildings.

Under the 2012 Energy Efficiency Directive it was established the following:

- EU countries must enforce energy efficient renovations to at least 3% of buildings owned and occupied by central government;
- EU governments should only purchase buildings which are highly energy efficient;
- EU countries must create their own National Energy Efficiency Action Plans, including long-term national building renovation strategies.

2.2 Energy performance certification

As mentioned above, the main goals of the energy certification system are implementing a classification that provides an accurate picture of the level of efficiency of a building and proposing strategies to enhance its energy performance. The proprietary or potential buyer/tenant of a building needs to be perfectly aware of its functionality to make informed decisions. Public buildings should set the example in terms of regular evaluations.

Following the developments in terms of European legislation, the *Sistema Nacional de Certificação Energética e da Qualidade do Ar Interior nos Edifícios* (SCE) was created in Portugal to enforce the new measures and approved in 2006. The SCE establishes guidelines to verify the set of rules has been applied and all new and old buildings have been evaluated. The assessment should be done by a qualified expert that will inspect the venture by the end of the project and construction phase. The evaluation of performance is based on the parameters defined in the *Regulamento das Características de Comportamento Térmico dos Edifícios* (RCCTE) (Pedrosa, 2009). When the project is successfully evaluated, the expert provides a *Declaração de Conformidade Regulamentar* (DCR), which is needed for submitting a request for the construction license. Likewise, after evaluating the building, a *Certificado Energético e da Qualidade do Ar Interior* (CE) is issued. This document will be required for the usage permit of the new building or for a transaction process of an existing one. The certification works in a scale from A^+ (best performance) to G (worst performance) and features measure related to the improvement of the building's performance. There are nine ratings possible, such as A^+, A, B, B^-, C, D, E, F and G. For new buildings, the minimum rating consists of B^-. On the contrary, there is no requirement for existing buildings.

3 STATE OF THE ART

3.1 Comprehensive approach of the use of genetic algorithms in civil engineering

Genetic algorithms (GAs) have been widely preferred by many researchers to solve optimization problems related to the civil engineering field (Pezeshk et al, 2002). Generally, a common civil engineering optimization problem consists of establishing variables that portray as close as possible the behavior of a building or structure; constraints that meet specific requirements imposed by regulations and the minimization of two opposed objectives, such as: speed of construction and cost, indoor discomfort and energy consumption. However, we may want to maximize one objective (structural resistance) and minimize the other (cost of the sections). The algorithm itself will have to convert a minimum problem to a maximum problem, since traditional genetic algorithms are only designed to run maximization problems.

The genetic approach works in the following distinctive ways compared to traditional algorithms (Pezeshk et al., 2002; Caldas and Norford, 2003):

- GAs work by improving an initial sizable population of solutions instead of operating on a single potential solution, which allows for a more diverse analysis and more case studies;
- GAs operate with a coding set of variables rather than the variables themselves, which means that there will be as many single variable codings as the number of variables defined in the problem, created through the concatenation of a binary string of specific length. The length will specify its range and precision. A new population will be established by decoding the individuals in the previous solution;
- GAs are able to analyze randomly ordered data;
- GAs are based on a probabilistic transition scheme instead of gradient information;
- GAs are efficient with discrete design variables;
- GAs are easily configured and intuitive for designers;
- GAs do not need a clear affiliation between the objective functions and the constraints. The value of the objective function will be penalized if any of the restrictions suffer infraction throughout the analysis;
- GAs allow for multiple load cases, such as the Multiobjective Problem.

These features make the genetic algorithm an ideal method for problem-solving in civil engineering design. Most of the traditional algorithms are only suited for the analysis of continuous design variables, since the search for local optimal solutions for discrete variables is not effective (Rajeev and Krishnamoorthy, 1992). Especially in structural optimization problems, the formulation will often require discrete design variables, which immediately excludes traditional algorithms.

3.2 Energy optimization problems solved by genetic algorithms – Related research

As explained above, GAs are a well-suited tool to solve a diverse set of civil engineering problems (Coley and Schukat, 2002), including the ones pertaining to the energy efficiency field. The focal point of this section is to present an overview of recent developments regarding the use of GAs in energy optimization. These problems have shown that GAs are able to provide high quality solutions and influenced the choice of the GA as the analytical algorithm for this work.

Wright et al (2002) conducted a study focused on determining the quality of the solutions generated by a multiobjective genetic algorithm for two different problems: the first one opposed the minimization of energy cost and maximization of zone thermal comfort and the second one used the minimization of capital cost and energy cost as objective functions. The three design parameters adopted were the operating cost of the HVAC system over a design day, the maximum thermal discomfort during occupancy for the design day and the capital cost of the construction and the HVAC system. They concluded that the multiobjective genetic algorithm had demonstrated a good performance for the energy cost – zone thermal comfort analysis and a subpar performance for the energy cost – capital analysis.

Caldas and Norford (2003) studied the advantages of the use of GAs instead of other optimization methods in the field of building design and tested the application of GAs in three different case studies: optimization of the building envelope to minimize HVAC, lighting systems and construction costs; optimization of building form; and optimization of the design and operation of HVAC systems. In comparison to the solutions found through an exhaustive search conducted with a backtracking algorithm, they were able to successfully generate a set of near-optimal solutions for all the case studies. They concluded that GAs are suited to handle several energy efficiency problems, such as optimization of wind driven ventilation and daylight, optimization of HVAC systems to reduce electrical power during peak-demand periods and optimization of the building form.

Wang et al. (2005) wrote a guideline that aimed to assist professionals in green building design through optimization. The multiobjective optimization model is explained thoroughly, with instructions on how to select objective functions, variables and constraints at the conceptual design stage that have an impact on the building's performance. A life cycle assessment is conducted to measure the expanded cumulative energy consumption of the model based on a single-story office building in Canada. Finally, the optimization is simulated and the authors concluded that using a GA provides good convergence of results and high quality solutions. In addition the following conclusions were taken: (i) the optimal wall type is a steel-frame wall for all the solutions in the Pareto frontier; (ii) an increase of insulation reduces the operational energy consumption; (iii) the optimal building orientation is zero and the optimal window ratio is 20%; and (iv) the rectangular shape with long side towards south is recommended to benefit energy performance.

Athienitis and Charron (2006) studied a solar-optimized building design in order to find the parameters with the most influence on the energy performance of net zero energy solar homes in Canada. They used a GA simulated on TRNSYS and concluded that a multiobjective optimization approach provided superior results compared to the traditional trial-and-error method. The optimal mass thickness varies depending on wall composition and material properties. Comfort levels inside the building are directly correlated to changes in south-facing windows, the thermal mass and the heating system.

Yi and Malkawi (2009) created a new methodology that enables the definition of building forms through the hierarchical relationship between geometry points, breaking the restrictions imposed by simple forms. The designer is granted the possibility of experimenting with complex forms, thus generating more possibilities to test. The analysis of the model was conducted by a merge of a computational GA simulation and energy performance combinations run by EnergyPlus. The optimal solution managed to reduce the heating load per volume by 12%, demonstrating the effect of the building form and how it can be improved with less effort through an optimization analysis.

Tuhus-Dubrow and Krarti (2010) studied the impact of building shape as a design variable with the aim of minimizing energy use and lifecycle cost, in comparison to other criteria such as orientation, insulation, windows area, glazing type, infiltration rate and thermal mass. An optimization analysis was performed on a Building America benchmark home in several US cities, aided by the combination of a computational GA simulation and DOE-2 (building energy analysis software). They concluded that rectangular and trapezoidal shaped buildings consistently have the best performance (lowest life-cycle cost) across five different climates; compared to L, T, U, H and cross shapes.

Shi (2011) investigated the optimal insulation strategy in order to minimize the space conditioning load of an office building located in China through the control of the insulation thickness of the walls. As a constraint, the insulation usage was kept at minimum throughout the case study. The multiobjective problem was simulated on modeFRONTIER and EnergyPlus. Shi concluded that the algorithm was capable of setting up well-defined Pareto frontier in a reasonable number of runs and that insulation had a clear impact on the performance of the building.

Bichou and Krarti (2011) studied the building design features that minimize the life cycle costs. The buildings featured in the case study were located in several parts of the United States. The researchers used three different simulation approaches: the Genetic Algorithm, the Particle Swarm Algorithm (PSA) and the Sequential Search algorithm. They concluded that the GA and PSA were more effective, since they needed less computational effort to provide optimal solutions. The study estimated that relying on optimal selection can reduce life cycle costs by 10–25%. The effectiveness depends on the climate and type of homes.

Horikoshi et al. (2012) analyzed the link between the building shape and interior zoning design as main factors in the minimization of the dependency on air conditioning and lighting systems to maintain the comfort of the building. The case study was performed on a city hall in Tokyo and simulated by the Energy Specific Unit Management tool. Building core arrangement, aspect ratio, building direction and window surface ratio were used as variables. They concluded that the window surface ration is responsible for a moderate reduction in lighting energy and great increase in air-conditioning demands. The authors proved that different core arrangements have heterogeneous lighting and AC needs.

4 INTRODUCTION TO OPTIMIZATION THEORY

This chapter introduces the theoretical concepts that serve as basis for the DesignBuilder's optimization tool. The optimization module uses a Non-Dominated Sorting Genetic Algorithm (NSGA-II), which constitutes a type of Multiobjective Evolutionary Algorithm, to generate a set of solutions that meet the design objectives.

4.1 Non-Dominated Sorting Genetic Algorithm (NSGA-II)

A genetic algorithm is an adaptive heuristic search algorithm that applies an analysis setup for all the variables akin to the natural selection process of evolution (Mitchell, 1996). In other words, the strings with the best characteristics will be chosen from the initial population of the study and passed through each iteration until an acceptable solution is reached. Each string encompasses a series of attributes that represent the values of the design variables for a particular solution.

The execution of a GA can be summarized as three different sequential operations (Pezeshk et al., 2002), such as:

1. Encoding of variables

The process of encoding converts information from a source into symbols in order to perform data transmission. On the contrary, decoding is the reverse process, which means converting code symbols back into the initial form. Both continuous and discrete design variables can be encoded to ease the computational effort to analyze the optimization problem (Alajmi and Wright, 2014). The most common strategy for encoding is turning the design variables into a binary chromosome, by assigning representative bits to each specific variable. Overall, GAs operate with a coding set of variables rather than the variables themselves. By the end of each simulation, a new population will be established by decoding the individuals in the previous solution.

2. Fitness assignment

Fitness of a string is the property that measures the performance of the design variables according to the previously established criteria in the beginning of the problem (objective functions and constraints). The newly created population of solutions will be ranked based on

the fulfillment of the objective functions, in a scale from "best" to "worst" solution. The performance of a solution will be penalized proportionally if it fails any of the constraints and hampered from the reproduction process through the action of penalty functions. This hierarchization process is called a stochastic ranking. The stochastic ranking attributes a probability of being chosen as a parent string for the next generation to each string of the current population in analysis. The probability is strictly based on the string's fitness (Pezeshk et al., 2002).

3. Selection of solutions

The selection operator is responsible for choosing the acceptable solutions from the current population that will serve as parent strings to form the next iteration of solutions. The first generation relies on a pseudo random number operator (Pezeshk et al., 2002) to create the initial population. Afterwards, a tournament operator will choose the winner solutions of the following populations (Alajmi and Wright, 2014). The manner in which the selection process is conducted means that the best set of characteristics will be assigned high probabilities of surviving in the next generation and increase their presence, while poor set of characteristics will be assigned low probabilities of continuing the process and likely dismissed, similar to the survival of the fittest.

A multiobjective problem is a multiple criteria decision problem that aims to solve more than one objective function at the same time (Talbi, 1965). Generally, the problem is formulated as the minimization of various objective functions, so, if an objective function is to be maximized, the algorithm will minimize its counterpart. Thus, the problem can be formulated as:

$$\min\big(f_1(x), f_2(x), \dots, f_k(x)\big) \quad s.t.\, x \in X \;;\; k \geq 2 \qquad (1)$$

The NSGA-II is an improved version of the original Non-dominated Sorting Genetic Algorithm introduced by Srinivas and Deb in 1994, with the goal of creating an alternative to traditional methods that tried to solve multiobjective optimization problems by scalarizing the objective vector into a single objective (Srinivas and Deb, 1994). In 2002, the NSGA-II was conceived through the joint effort of Deb, Pratap, Agarwal and Meyarivan; in order to resolve the main of flaws of the NSGA process (Deb et al., 2002), such as: high computational complexity of non-dominated sorting, lack of elitism and the need for specifying the sharing parameter σ_{share}.

The distinctive features of the NSGA-II can be summarized as (Open Engineering, Multiobjective optimization and Genetic algorithms):

- A sorting non-dominated procedure where all the individual are sorted according to the level of non-domination of the objective vectors;

- The implementation of elitism which has the ability to store all non-dominated solutions and strengthen the convergence properties of the algorithm;
- The adoption of automatic mechanics based on the crowding distance in order to assure diversity and a broad set of solutions;
- Constraints are implemented using a modified definition of dominance without the requirement of enacting penalty functions.

4.2 Pareto optimal solutions

A generic multiobjective optimization solver searches for non-dominated solutions that correspond to trade-offs between all the objectives. A non-dominated solution is reached when none of the objective functions can be improved in value without worsening some of the other objective values. These are called decision or objective vectors.

Typically, there is not a single solution that simultaneously optimizes each objective for a non-trivial Multiobjective operation (Openeering, Multiobjective optimization and Genetic algorithms). The several solutions obtained by the end of the process are called Pareto optimal solutions due to the fact that conflicting objective functions cannot be improved in value without degrading some of the other objective values. The image of the Pareto set in objective space is called Pareto front and is illustrated in Figure 4.1.

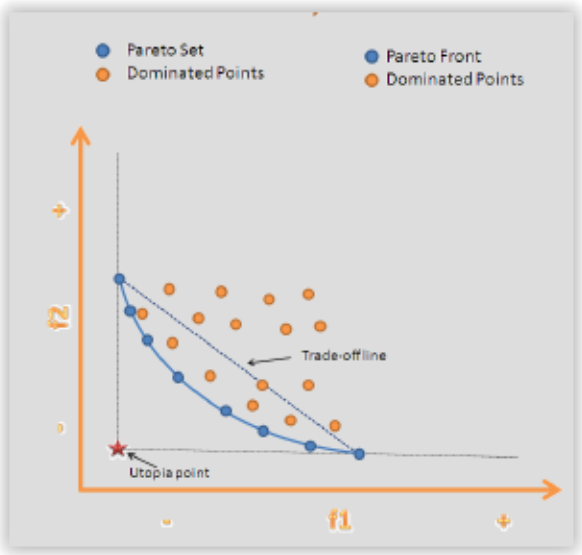

Figure 4.1 – Pareto front with a convex shape (Openeering)

After reaching the set of acceptable solutions, there are different methods for solving the problem and selecting the preferred solution. In this case, the computer program follows an "a posteriori" method, where a representative set of Pareto optimal solutions is presented through

graphical and numerical outputs to the user and the human decision maker is responsible for choosing the most appropriate one according to his scale of priorities.

Two types of Pareto fronts can arise when solving multiobjective optimization problems: convex shape and non-convex shape. In the case of good convergence, it is expected that the Pareto front will most likely assume a convex shape for the problem. The convex front generates a superior trade-off compared to the linear combination of the original objectives. In other words, if the decision maker decides to forfeit an optimal solution in detriment of another, the gains of performance for the preferred objective function will account for the losses of performance of the undervalued target, in the same proportion.

4.3 Simulation parameters

Before the analysis, several parameters need to be set to calibrate the simulation of the reproduction process. The quantity, quality and convergence of the solutions in the Pareto front are directly correlated to the selection of parameters (Pezeshk et al., 2002). Moreover, the computational effort and running time required to reach the solutions will vary according to the chosen settings.

4.3.1 Population size

Population size is the number of individuals that can be tested in a simulation sample and will be responsible for the breeding of new generations. These individuals will be the domain of the search space. The bigger the population size, the more different solutions may exist within the same generation. However, the increase of the population size will boost the computational effort and running time.

4.3.2 Number of generations

The number of generations is the number of simulation tests that will be run by the algorithm. In other words, it means the amount of completed iterations. In the same vein as the population size, the number of generations will determine the time/computing resources required to complete the analysis. If convergence is achieved early on, increasing the number of generations will not be beneficial for the analysis.

4.3.3 Mutation rate

The mutation rate grants the possibility of non-existing characteristics emerging in the information that is transmitted from parent strings to their correspondent children strings. The creation of new features that are not present in the previous generations expands the analysis into new territories of the search space, providing evolutionary advantages that will enhance the performance of the next generations. Nonetheless, increasing the mutation rate will impair the convergence of the problem. The default individual mutation probability used in DesignBuilder is 1.0.

4.3.4 Crossover

Crossover is a recombination operator that controls the procedure wherein parent strings are split into various segments and a child string is produced by swapping pieces of information between the two individuals. Therefore, crossover allows for two parent strings to randomly supply their desirable features and create two offspring that have the potential to perform better than their ancestors. The default crossover rate used in DesignBuilder is 0.9.

4.3.5 Tournament size

The tournament size is the scope of a random sample taken in the current generation, where the best solution will be picked by the tournament operator as a participant in the reproduction process. The default tournament size in DesignBuilder is 2.0.

5 THE OPTIMIZATION PROBLEM

In this chapter, all the stages of setting up the optimization problem will be clarified. Initially, the focus will lie on the complete contextualization of the case study, such as: overview of the energy performance of lightweight steel buildings, outline of the properties of the model and review of the climatic zones. Consecutively, a pre-optimization evaluation will be conducted on the reference models, to assess their performance in terms of energy and thermal performance for further comparison. Finally, a parametric analysis will be run in order to identify the design variables with more impact on the model and the assumptions behind the choice of the optimization settings will be explained.

5.1 Characterization of lightweight steel buildings

Light steel framing is a method that relies on cold-formed steel as the main structural element of the building, which provides better structural reliability for a lower self-weight and easiness of the construction process. The method was developed by the American Iron and Steel Institute and published in 1997. In Europe, there has been a growing market for this type of solution applied to lower height buildings, with a maximum of three floors. The replacement of traditional concrete and brick masonry with lightweight steel brings numerous advantages to the construction and usage process of small residential buildings (Lawson, 2009) such as:

- Cost
- Speed of execution
- Thermal performance
- Acoustic performance
- Seismic performance
- Sustainability
- Fire safety
- Structural rehabilitation
- Framework and building in height

In terms of energy efficiency, there are real benefits associated with light steel framing, despite the fact that the steel itself doesn’t have any effect as a heat insulator. A LSF wall

consists of a very thin light steel section, polymeric mortar, extruded polystyrene, stone wool, plasterboard, oriented strand board panels and waterproof paint, as illustrated in Figure 5.1.

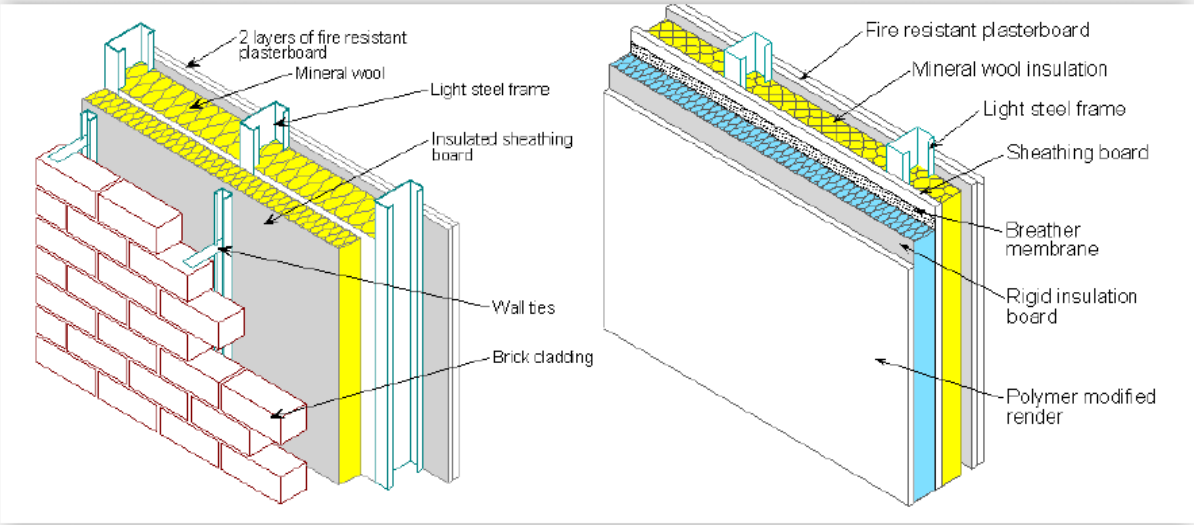

Figure 5.1 – (a) Brick wall connected to a LSF; (b) Insulating material in the interior of the LSF (Pires, 2013)

The advantages of light steel framing related with energy efficiency are the following for climates with low thermal amplitude during the day (Pires, 2013):

- Reduction of thermal bridges

The surface of the wall exposed to thermal bridges corresponds to a maximum value of 0,375%, which means that 99,625% of the wall's area is completely insulated.

- Heat insulation

Studies have shown that a conventional residential home constructed with concrete and brick masonry would need a brick wall with 86 cm of thickness just to provide the same level of heat insulation as a LSF wall with 5 cm of thickness, due to the thermal conductivity properties of the used materials.

- Minimization of natural ventilation losses

The airtight building envelope limits incoming air to controlled ventilation which allows for increased control over indoor air quality, reducing energy losses caused by natural ventilation.

- Elimination of thermal inertia

All the components of the LSF wall are very thin materials, with low density and volumetric heat capacity, which nullifies the thermal inertia effect. This reduces energy waste, since the potency needed to maintain the same temperature in a room decreases with insignificant

thermal inertia, combined with the good insulation provided by the LSF wall. For swing climates, with a daily variation of temperature superior to 10^0C, this would be considered a disadvantage.

5.2 Case study: General description

The case study will be based on the analysis of a residential building, consisting of a two-story house with a basement, composed of three bedrooms for a single family. The ground floor is composed by a living room, kitchen, bathroom and it is connected to the first floor by a flight of stairs. The living room is facing the Southern hemisphere to maximize the degree of sunlight exposure, while the kitchen is placed on the Northern one. The top floor displays a suite with a private bathroom, two other bedrooms and shared bathroom in the common area. The total area of the building consists of 194,46 m^2. The structural system of the building is a Light Steel Framing structure designed according to the *Eurocode 1993: Design of steel structures*. The arrangement of all the divisions is displayed on the Appendix section. The building orientation is 345º relative to North. Additional information regarding the characterization of the building's components can be found in the Appendix section (Tables A.1 to A.9).

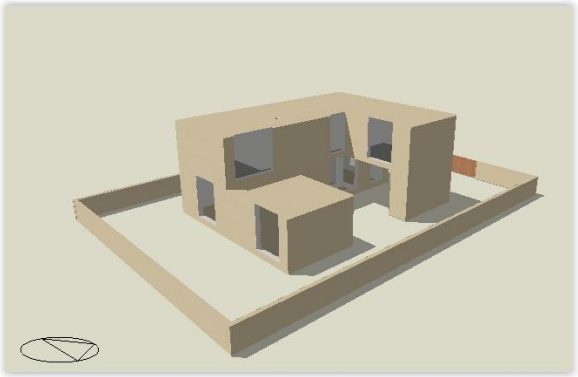

Figure 5.2 – 3D view of the model

The heating setpoint temperature of the house is 20^0C, while the cooling setpoint temperature remains 25^0C, in order to meet the requirements established for inside air temperature by the 2010 Energy Performance of Buildings Directive (2010/31/EU). The mechanical ventilation consists of 0,60 ac/h (explanation in section 5.7.2); the electric heating system has a COP of 1,00 (Mitsubishi Electric, http://www.mitsubishielectric.ca/en/hvac/zuba-central/powerful_savings.html) and it will be turned on during the Winter (Northern Hemisphere); the electric cooling system has a COP of 3,20 (Powerknot, http://www.powerknot.com/how-efficient-is-your-air-conditioning-system.html) and it will be turned on during the Summer (Northern Hemisphere). The domestic hot water system is instantaneous hot water only, consumes electricity, has a COP of 0,85 (Energystar.gov,

https://www.energystar.gov/ia/partners/prod_development/new_specs/downloads/water_heaters/ElectricTanklessCompetitiveAssessment.pdf) and can be used 24/7. These HVAC settings aim to portrait a standard home system with medium energy performance.

The location of the model will vary according to three different Köppen climatic zones: Csa (Model 2 located in Rome, Fiumicino), Csb (Model 1 located in San Remo) and Cfb (Model 3 located in Berlin, Dahlem); covering most of Central and Southern Europe as described in the following sub-section.

5.3 Köppen climate classification

The Köppen climate classification is a vegetation-based empirical climate classification system (Arnfield, 2016) built on the premise that each climate zone can be traced to a specific set of vegetation characteristics, since biomes are controlled by the manifesting climatic conditions. Therefore, it is possible to infer that the climatic conditions will determine what types of plants grow in a certain region. Climate zone boundaries have been established according to different factors that influence the distribution of vegetation in Earth's surface, namely: average annual temperature and precipitation, average monthly temperatures and precipitation and the seasonality of precipitation (McKnight and Hess, 2000).

As indicated in Table 5.1, the chart divides terrestrial climates into five major types, represented by the capital letters A, B, C, D, and E. The C group exhibits a temperate/mesothermal climate and a lower case letter is attributed to the code to portrait the correspondent subtype of climate.

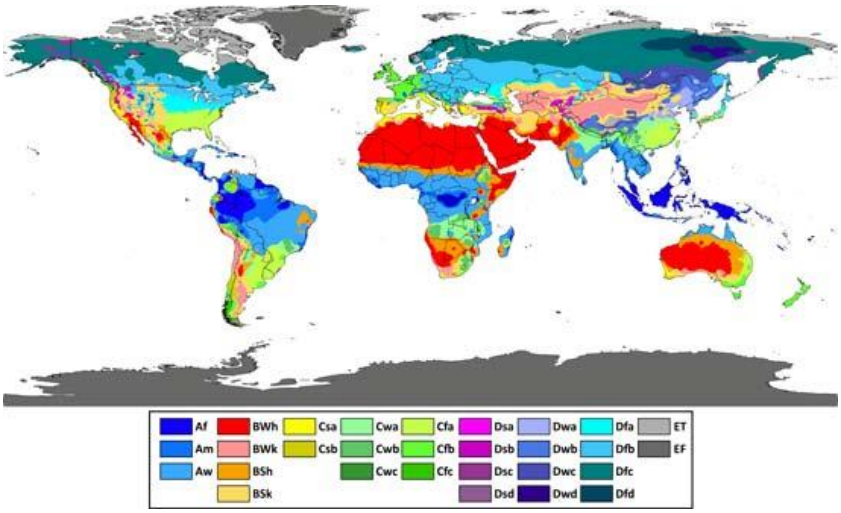

Figure 5.3 – Updated world map of the Köppen-Geiger climate classification (Encyclopaedia Britannica, 2016)

The three climatic regions selected for the case study can be described as the following:

- Csa: Temperate climate with dry and warm summer;
- Csb: Temperate climate with dry and temperate summer;
- Cfb: Temperate climate with humid and temperate summer.

Table 5.1 – Coding options for the C climate group (Encyclopaedia Britannica, 2016)

C			temperature of warmest month greater than or equal to 10 degrees Celsius, and temperature of coldest month less than 18 degrees Celsius but greater than –3 degrees Celsius
	s		precipitation in driest month of summer half of the year is less than 30 mm and less than one-third of the wettest month of the winter half
	w		precipitation in driest month of the winter half of the year less than one-tenth of the amount in the wettest month of the summer half
	f		precipitation more evenly distributed throughout year; criteria for neither s nor w satisfied
		a	temperature of warmest month 22 degrees Celsius or above
		b	temperature of each of four warmest months 10 degrees Celsius or above but warmest month less than 22 degrees Celsius
		c	temperature of one to three months 10 degrees Celsius or above but warmest month less than 22 degrees Celsius

5.4 Comfort levels analysis

The main goal of this thesis is to reduce the levels of energy consumption of a lightweight steel building. However, the study would not be complete without a detailed analysis of the comfort levels of the building, since there is a trade-off between energy consumption and discomfort experienced inside the building. This trade-off can be minimized by cutting the heating and cooling demands of the building as much as possible.

DesignBuilder operates under American regulations for comfort calculations. The ASHRAE 55 standard considers several factors (Mean radiant temperature, air speed, metabolic rate and clothing level) to formulate an admissible range for operative temperature and relative humidity; which can be consulted in the following figure:

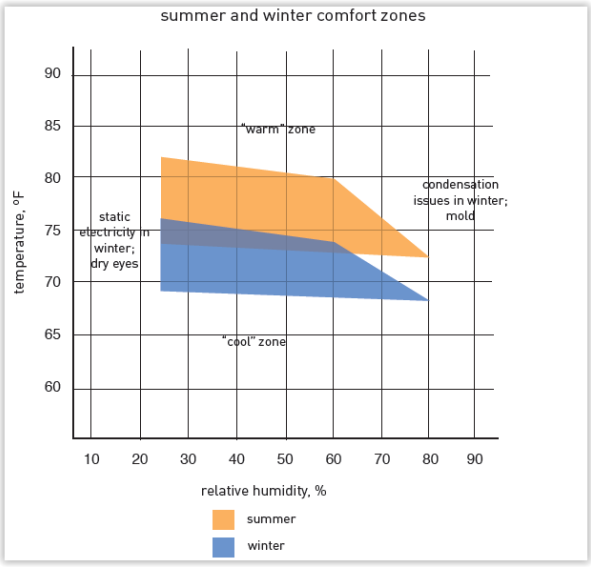

Figure 5.4 – ASHRAE 55 comfort zones (Boduch and Fincher, 2009)

Operative temperature is described as the uniform temperature of an imaginary black enclosure in which an occupant would exchange the same amount of heat by radiation plus convection as in the actual nonuniform environment; while relative humidity is the ratio of the partial pressure of water vapor to the equilibrium vapor pressure of water at a given temperature (ASHRAE Standard 55, 2013). The five parameters used to evaluate comfort levels are: discomfort hours ASHRAE 55 - all winter and summer clothes, average operative temperature for all summer, average operative temperature for all winter, heating degree hours and cooling degree hours.

In order to get the full picture of the breakdown of heating and cooling demands, the annual optimization results for discomfort hours must be split in two timeframes: the heating period ("all winter") and the cooling period ("all summer"). The "all summer" period is defined by DesignBuilder for the Cfb climate as running from April 1st to September 30th and the "all winter" period encompasses the timespan from January 1st and March 31st with the October 1st to December 31st timeframe; consequently making this an all-year analysis. Giving the differences in metrological conditions, for the Csb and Csa climates, the "all summer" period runs from May 1st to October 31st and the "all winter" period encompasses the timespan from January 1st and April 30th with the November 1st to December 31st timeframe.

- "Discomfort hours ASHRAE 55 - all winter and summer clothes" (h)

This parameter is calculated through the sum of "Discomfort (hours)" results for all year, which can be obtained through the "Comfort" category after running an EnergyPlus annual simulation on the models. It represents number of hours when the operative temperature and

relative humidity of the building remain outside of the acceptable spectrum defined by the ASHRAE 55 requirements.

- "Average operative temperature for all summer" (ºC)

This parameter is calculated from the hourly data results for operative temperature, which can obtain through the "Comfort" category after running an EnergyPlus annual simulation on the models.

- "Average operative temperature for all winter" (ºC)

This parameter is calculated from the hourly data results for operative temperature, which can obtain through the "Comfort" category after running an EnergyPlus annual simulation on the models.

- "Heating degree hours (HDH)" (h)

This parameter is calculated through the sum of "Discomfort (hours)" results for all winter, which can be obtained through the "Comfort" category after running an EnergyPlus annual simulation on the models. It represents the number of hours when the operative temperature and relative humidity of the building infringe the established acceptable range for the winter comfort zone for each climatic region. Thus, reflecting the demand for heating energy to make up for the deficit and maintain the building operating comfortably for its users.

- "Cooling degree hours (CDH)" (h)

This parameter is calculated through the sum of "Discomfort (hours)" results for all summer, which can be obtained through the "Comfort" category after running an EnergyPlus annual simulation on the models. It represents the number of hours when the operative temperature and relative humidity of the building infringe the established acceptable range for the summer comfort zone for each climatic region. Thus, reflecting the demand for cooling energy to make up for the deficit and maintain the building operating comfortably for its users.

5.5 Analysis of reference models

A reference model is considered for each climate region and the energy demands of each model are indicated in this section. These results, which are not optimized, will be later used for further comparison with the results from the optimized models. The main objective is to lower the current energy consumption, without compromising the functionality of the building, so the results for "Total site energy" and "Discomfort ASHRAE 55 (all clo)" will be the focal point to assure the quality of the simulations (Table 5.1). The details of the design variables used in each reference model can be consulted in the Tables 5.2 to 5.4, in order to make the comparison with the optimization choices later on.

5.5.1 Pre-optimization results

Regarding the pre-optimization comfort levels, it is clear that the main deficit in terms of energy demands falls on the winter comfort zone for all the reference models and there is a lot of room for improvement (Table 5.1). For the Csb and Csa climates, HDH more than double CDH; while for the Cfb climate, HDH actually triple CDH. The average operative temperature for the Csb, Csa and Cfb reference models is the following (Tables 5.2):

- Csb: 19,68^0 C (all winter) and 23,95^0 C (all summer);
- Csa: 19,49^0 C (all winter) and 24,02^0 C (all summer);
- Cfb: 18,24^0 C (all winter) and 21,93^0 C (all summer).

The annual simulation results for the pre-optimized reference models are the following:

Table 5.2 – Initial results (Model 1,2 and 3)

Pre-optimization results: Analysis of reference models			
Initial Features	Model 1	Model 2	Model 3
Climate	Csb	Csa	Cfb
Total site energy (kWh)	14330,31	17168,79	24353,88
Discomfort ASHRAE 55 (all clo) (h)	3092	3279	4179
CDH - All Summer (h/year)	857	972	1045
HDH - All Winter (h/year)	2234	2311	3135
OT average- All Summer (ºC)	23,95	24,02	21,93
OT average- All Winter (ºC)	19,68	19,49	18,24

The design variables for each reference model are the following:

Table 5.3 – Design variables (Model 1)

Model 1	
Climate	Csb
Glazing type - Exterior	Simple window with 6 mm thickness - No glazing
Glazing type - Interior	Clear glass with 3mm thickness - No glazing
Infiltration (ac/h)	0,06
Insulation - External wall construction	LSF with 120 mm insulation thickness
Insulation - Flat roof construction	Roof with 100 mm insulation thickness
Building orientation (ºC)	345

Table 5.4 – Design variables (Model 2)

Model 2	
Climate	Csa
Glazing type - Exterior	Simple window with 6 mm thickness - No glazing
Glazing type - Interior	Clear glass with 3mm thickness - No glazing
Infiltration (ac/h)	0,06
Insulation - External wall construction	LSF with 120 mm insulation thickness
Insulation - Flat roof construction	Roof with 100 mm insulation thickness
Building orientation (º)	345

Table 5.5 – Design variables (Model 3)

Model 3	
Climate	Cfb
Glazing type - Exterior	Simple window with 6 mm thickness - No glazing
Glazing type - Interior	Clear glass with 3mm thickness - No glazing
Infiltration (ac/h)	0,06
Insulation - External wall construction	LSF with 120 mm insulation thickness
Insulation - Flat roof construction	Roof with 100 mm insulation thickness
Thermal mass construction - Exterior	None
Thermal mass construction - Interior	Painted wooded window frame

5.5.2 Pre-optimization comfort levels

The graphs demonstrating the yearly evolution of the operative temperature for each reference model are the following:

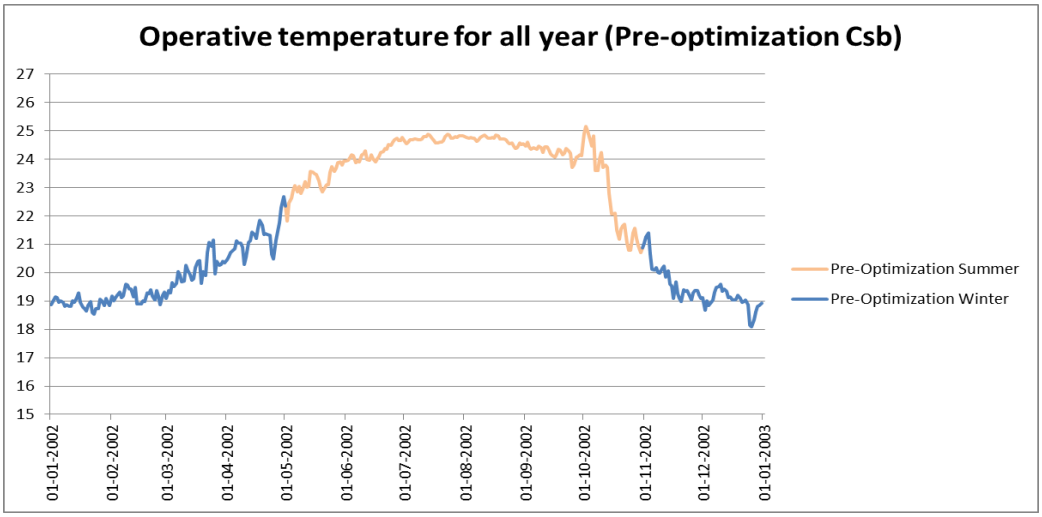

Figure 5.5 – Operative temperature for all year (Pre-optimization Csb)

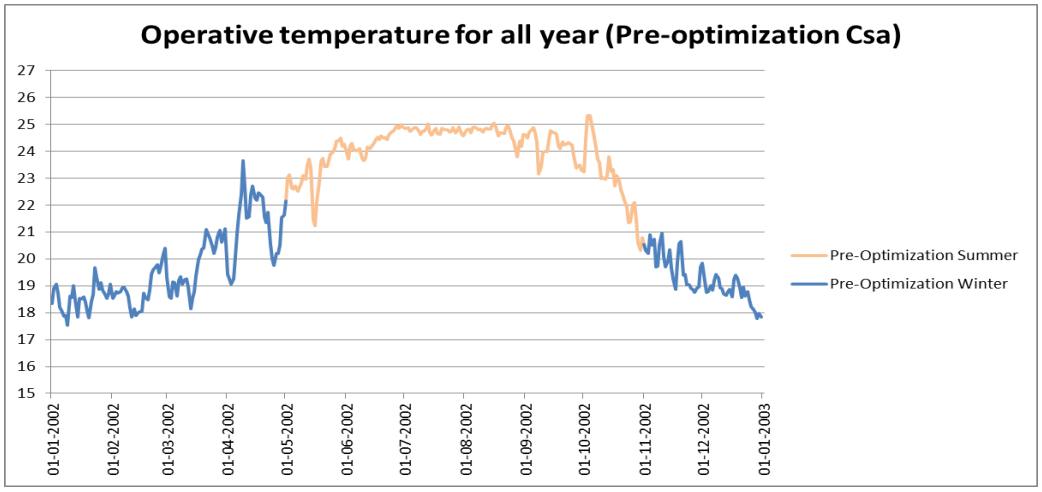

Figure 5.6 – Operative temperature for all year (Pre-optimization Csa)

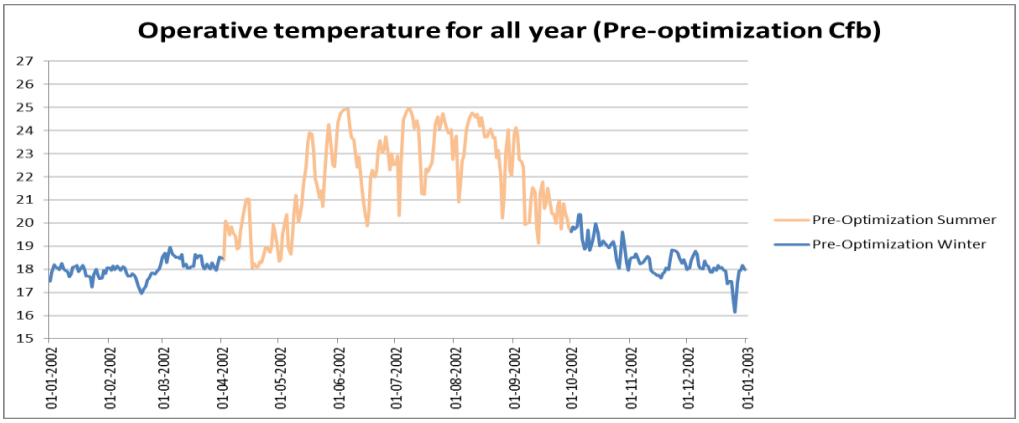

Figure 5.7 – Operative temperature for all year (Pre-optimization Cfb)

In order to get a more explicit perspective of the temperature swings for further comparison between the reference and optimized models, the “summer typical week” and “winter typical week” output will be displayed. The “summer typical week” runs from 22/06 to 28/06 for the Csb climate; 13/07 to 19/07 for the Csa climate and 17/08 to 23/08 for the Cfb climate. The “winter typical week” runs from 22/12 to 28/12 for the Csb climate and 27/01 to 02/02 for the Csa and Cfb climates.

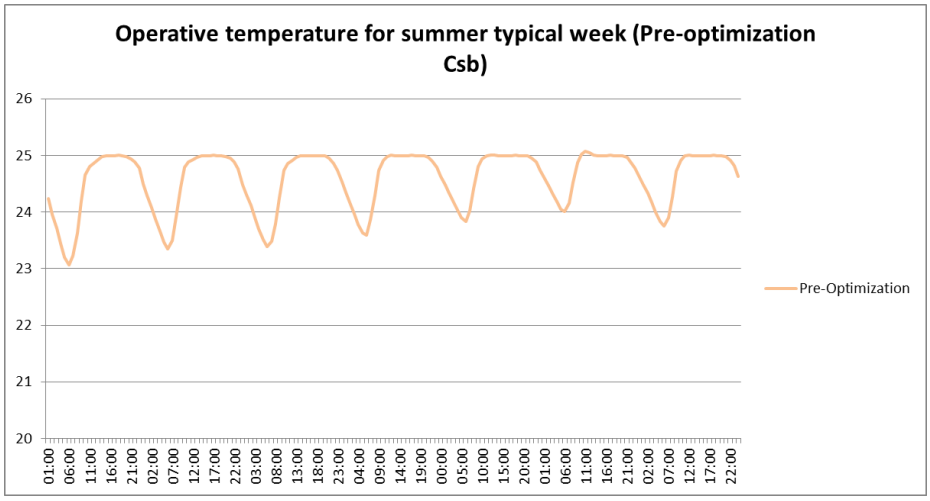

Figure 5.8 – Operative temperature for summer typical week (Pre-optimization Csb)

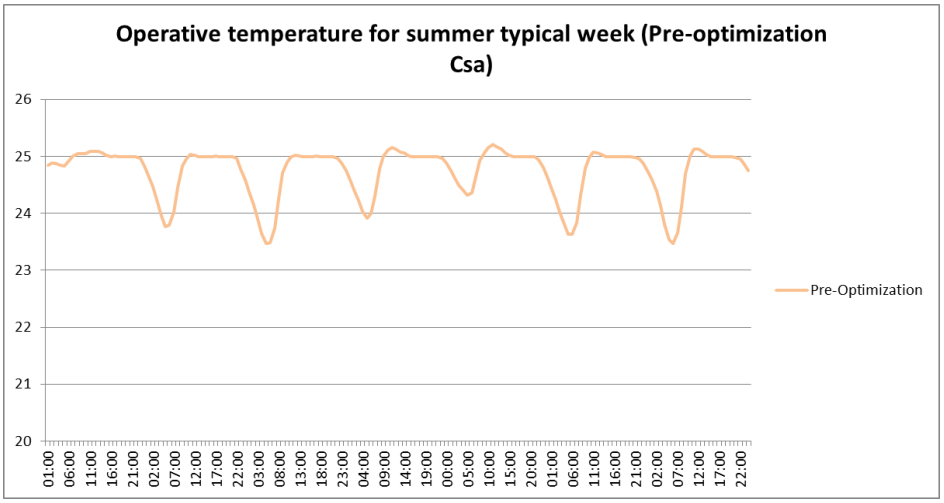

Figure 5.9 – Operative temperature for summer typical week (Pre-optimization Csa)

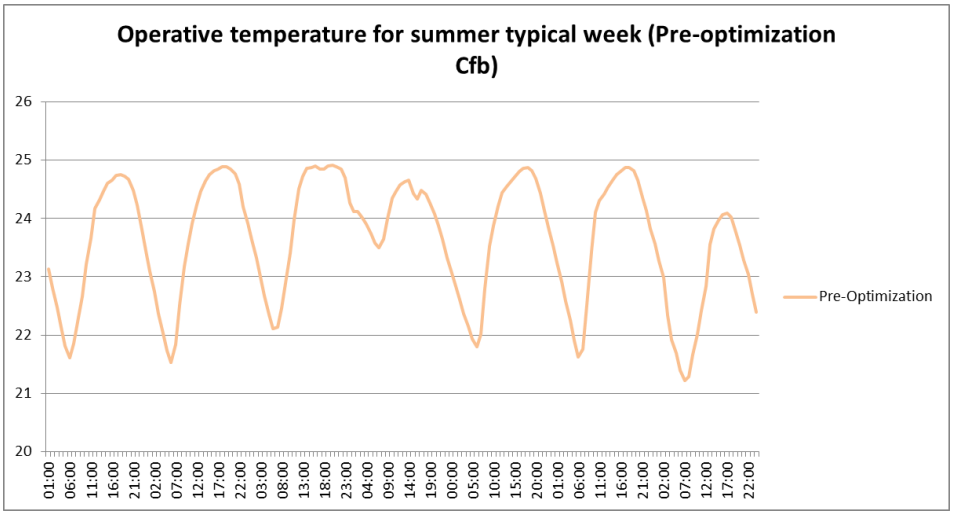

Figure 5.10 – Operative temperature for summer typical week (Pre-optimization Cfb)

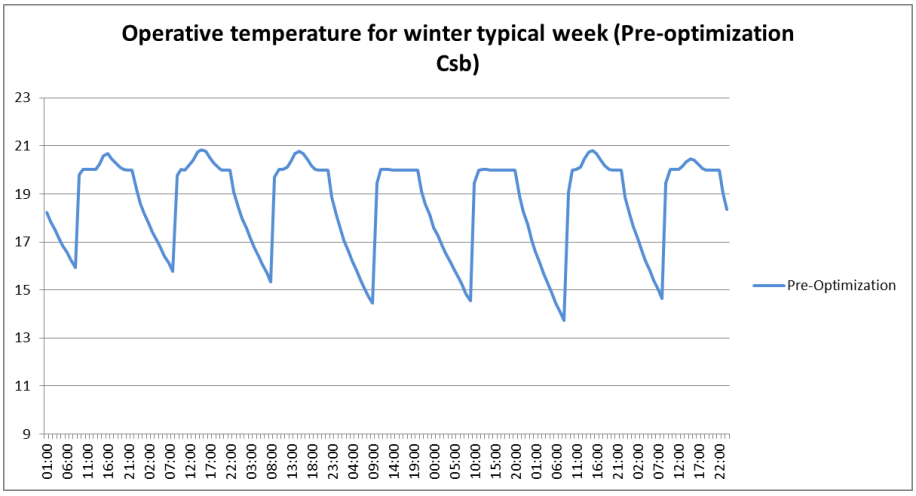

Figure 5.11 – Operative temperature for winter typical week (Pre-optimization Csb)

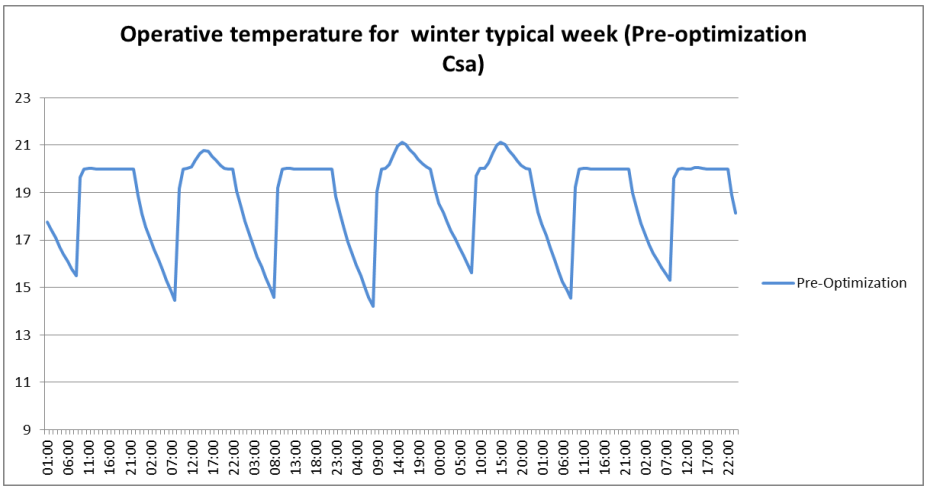

Figure 5.12 – Operative temperature for winter typical week (Pre-optimization Csa)

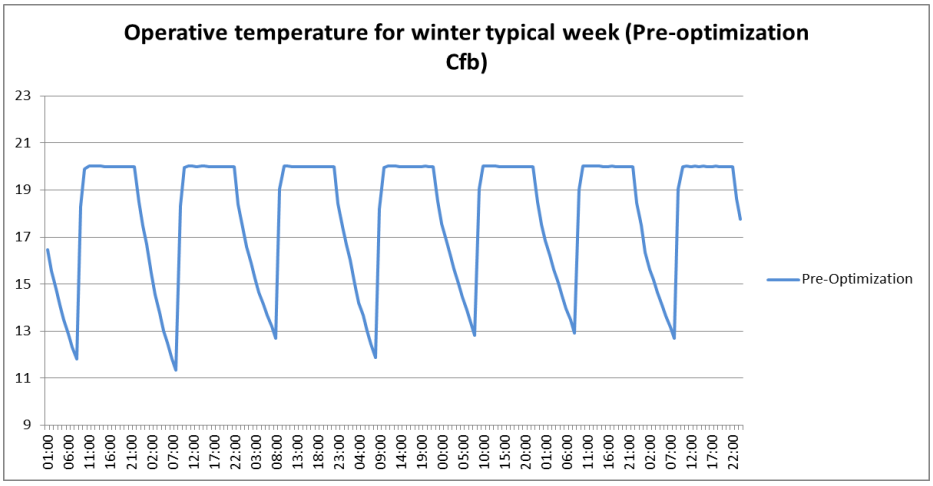

Figure 5.13 – Operative temperature for winter typical week (Pre-optimization Cfb)

5.6 Parametric analysis

In this section, a parametric analysis is performed in order to identify the most important design variables influencing the thermal behavior of the building.

5.6.1 Parameters that influence the energy performance of buildings

The strategies for reaching the optimal effect of the parameters mentioned in this section are suited for climates with low thermal amplitude during the day. However, most of them equally apply to swing climates, with the exception of the measures that seek the decrease of heat transfers.

- Orientation of the building

The orientation angle impacts the level of direct solar radiation gathered by the building façade, increasing the quantity of daylight and natural heating.

Ways of maximizing the effect of the orientation of the building:

Rotation to the south: The optimal building orientation for a rectangular house consists of a rotation of 30 degrees regarding the southern axis for the longest walls, providing the greatest energy savings in terms of heating and cooling (United States Air Force, 2001).

- Shape of the building

The shape factor means the ratio of building length to building depth. This element controls the level of exposition of the building façade. In other words, the volume to outer surface area ratio determines the level of heat losses and gains, accounting for 10 to 20% of the final energy demands (Danielski et al, 2012).

Ways of maximizing the effect of the shape of the building:

Compactness: The surface-area-to-volume ratio should be as low as possible to cause minimal heat transfers through the building.

- Building envelope

The building envelope encompasses all of the key elements of the building's shell that are responsible for keeping the climate control of the indoor environment regulated, such as the outer walls, roof, foundation, windows and doors. All this components combined end up working together as a physical barrier between the interior and exterior parts of the building, conditioning the energy transfers that take place. The thermal envelope is the heat flow

control layer. In cases of low efficiency of the thermal envelope, it can be responsible for up to 75% of building's energy losses (Hastings et al, 2007).

Ways of maximizing the effect of the thermal envelope:

Orientation of the building: The rooms with greater energy demands (sleeping and living rooms) should be located in the direction of the Southern hemisphere (Pacheco et al, 2012); while the divisions with less energy demands (bathrooms and storage rooms) should face the Northern hemisphere.

Exposed area of the building's surface: Decreasing the exposed area that has the ability of transferring heat to the exterior will result in lowering the energy demands of the whole building.

Thermal conductivity properties of the materials: Materials with low thermal conductivity will allow a decrease in heat transfers between the interior and the exterior.

- Windows

The glazing material of the windows has an overall heat transfer coefficient, at least, five times greater than the rest of the typical construction materials (Baker and Steemers, 2000), even in cases of good thermal performance, thus being the biggest contributor of the building envelope in terms of heat losses, around 30% of the total value (Roosa, 2010). These losses can happen in four distinctive manners (Button and Pye. 1993): thermal radiation exchanges between the glazing surface and the opaque surface of the building, air infiltration through the windows, air convection and conduction losses from the components of the windows. The energy balance is not entirely negative, since the windows compensate in terms of allowing solar energy reception for the building, which decreases the artificial lightning dependence.

Ways of maximizing the effect of the windows:

Area and orientation of the glazing: Most of the total glazing area (50% to 80%) should be concentrated in of the South front of the building, to capture the heating gains during the winter. However, a maximum of 40% of the total front should not be exceeded to avoid overheating during the summer months (Gonçalves et al, 1998). The glazing should be reduced as much as possible in the North, East and West fronts, since there are the most exposed to variations of temperature, especially during the winter.

- Shading

The use of shading devices has an impact in the form of controlling heating and lighting transfers throughout the year. There are two different types of equipment: inside and outside devices. Inside devices, such as blinds, rollers and curtains, are placed behind the glass and can only reflect part of the radiation, while the rest is absorbed and radiated into the building. Outside devices, like fins and overhangs, completely protect the window from exterior radiation, preventing the heat from ever getting into the room in the first place. Additionally, we can obtain extra shading from other buildings or surrounding vegetation.

Ways of maximizing the effect of the shading:

Position of the device: The apparatus should be positioned to completely allow low winter sun to be absorbed by the window while completely blocking the entire window from summer sun, in order to fix the heating balance.

Orientation of the device: The equipment is more effective while facing the South, compared to an increased reduction of performance while turned to the east and west façades (USC Department of Architecture).

Surrounding elements: The solar window (quantity of sunlight that a part of the building is exposed to given its placement) should be harnessed as better as possible; therefore the building needs to be placed in a way that being entirely shaded or cold at certain times of day is avoided. On the contrary, the surrounding elements can be used to provide beneficial cooling. Vegetation strategically planted can save up to 30 % of the building's total energy requirement (Olgay, 1963).

- Thermal insulation

A thermal energy transfer always occurs when there is contact between spaces with different temperature levels. Thermal insulation of a building refers to the capability of its components to provide a reduction of heat transfers, by decreasing thermal conduction. Heat transfers happen at a diminished rate across materials of low thermal conductivity, which is ideal to lessen thermal fluctuations and maintain a comfortable temperature inside of the building.

Ways of maximizing the effect of the thermal insulation:

Choice of materials: Materials with high thermal resistance (R-value) and low thermal conductivity (U-value).

Thickness of materials: Increasing the thickness of the same material will raise its contribution to the insulation process.

Placement of the insulation: Exterior surface of the thermal mass, such as external coating of the walls, roof and pavements. Window insulation film can also be applied.

Solar Heat Gain Coefficient (SHGC): Solar heat gain through windows is a significant factor in determining the cooling load of buildings. A high coefficient causes high heat gain, while a low coefficient decreases heat gains and keeps the cooling demands lower.

- Natural Ventilation

Natural ventilation, also known as passive ventilation, is the procedure of supplying air to and removing air from an indoor space without aid of any mechanical systems. A difference in pressures between the building and the outside area causes the outdoor air flow, which is called wind driven ventilation. Openings on the building perimeter, such as windows, will be responsible for controlling the outdoor air flow. Ventilation of the internal spaces of the building affects the thermal comfort experienced by its residents, by providing natural cooling, and it is detrimental to the renovation of the indoor air for removal of excessive water vapor.

Ways of maximizing the effect of the natural ventilation (National Institute of Building Sciences):

Orientation of the ridge: The ridge of the building should be located perpendicular to the summer winds.

Narrowing of naturally ventilation zones: The width of naturally ventilation zone should never exceed a maximum of 13,70 m.

Architectural options: Using clerestories on the building's configuration and vented skylights.

Location of the openings: The windows should be facing each other across the room to maximize air mixing and minimize flow obstruction. Every room should have two separate openings for air supply and exhaust. The exhaust system will be placed high above inlet to maximize the stack effect (movement of air particles due to air buoyancy).

5.6.2 Variation of main parameters

After thorough revision of literature on energy efficiency, the parameters that have demonstrated the ability of influencing the energy performance of buildings were singled out in the previous section of this work. In an optimization analysis, it is very important to choose settings that allow for an efficient computational effort to solve the problem. Thus, only the parameters that had a medium or higher impact on the energy consumption (total site energy) and operative temperature control of the model were selected for further testing. All the variables were applied at a building level. The following variables had to be tested through a parametric analysis conducted on Design Builder to measure their performance:

- Glazing type

This variable introduced eighteen different options for analysis, such as:
1 – Vertical glazing, 0%-40% of wall, U-0,35 (1.99), SHGC-0.40;
2 – Vertical glazing, 0%-40% of wall, U-0,35 (1.99), SHGC-0.45;
3 – Vertical glazing, 0%-40% of wall, U-0,40 (2.27), SHGC-0.40;
4 – Vertical glazing, 0%-40% of wall, U-0,40 (2.27), SHGC-0.45;
5 – Vertical glazing, 0%-40% of wall, U-0,45 (2.56), SHGC-0.40;
6 – Vertical glazing, 0%-40% of wall, U-0,45 (2.56), SHGC-0.45;
7 – Vertical glazing, 0%-40% of wall, U-0,50 (2.84), SHGC-0.40;
8 – Vertical glazing, 0%-40% of wall, U-0,55 (3.12), SHGC-0.40;
9 – Vertical glazing, 0%-40% of wall, U-0,60 (3.41), SHGC-0.25;
10 – Vertical glazing, 0%-40% of wall, U-0,65 (3.69), SHGC-0.25;
11 – Vertical glazing, 0%-40% of wall, U-0,70 (3.97), SHGC-0.25;
12 – Vertical glazing, 0%-40% of wall, U-0,75 (4.26), SHGC-0.25;
13 – Vertical glazing, 0%-40% of wall, U-0,80 (4.54), SHGC-0.40;
14 – Vertical glazing, 0%-40% of wall, U-0,80 (4.54), SHGC-0.45;
15 – Vertical glazing, 0%-40% of wall, U-0,85 (4.83), SHGC-0.40;
16 – Vertical glazing, 0%-40% of wall, U-0,90 (5.11), SHGC-0.25;
17 – Vertical glazing, 0%-40% of wall, U-1,10 (6,25), SHGC-0.25;
18 – Vertical glazing, 0%-40% of wall, U-1,20 (6,81), SHGC-0.25.

- Building orientation

The minimum value studied for building orientation was 0 degrees, while the maximum was 345 degrees, with steps of 15 degrees in between.

- Window to wall %

The minimum value studied for window to wall % was 10,00%, while the maximum was 90,00%, with steps of 10,00% in between.

- Window blind type

This variable introduced ten different options for analysis, such as:
1 – Blind with high reflective slats;
2 – Blind with medium reflective slats;
3 – Blind with low reflective slats;
4 – High reflectance – low transmittance shade;
5 – Medium reflectance – medium transmittance shade;
6 – Medium reflectance – low transmittance shade;
7 – Low reflectance – high transmittance shade;
8 – Low reflectance – medium transmittance shade;
9 – Low reflectance – low transmittance shade;
10 – None.

- Local shading type

This variable introduced six different options for analysis, such as:
1 – 0.5 m Overhang;
2 – 1.0 m Overhang;
3 – 1.2 m Overhang;
4 – 1.5 m Overhang;
5 – 2.0 m Overhang;
6 – No shading.

- Insulation – External wall construction

This variable introduced seven different options for analysis. All the layers have remained the same, except for the thickness insulating layer, which was tested for multiple combinations:

Table 5.6 – Thickness options for the insulating layer of the external walls

External walls - Stone wool	
Thickness (mm)	Variation
120	0
144	+20%
168	+40%
216	+80%
96	-20%
72	-40%
24	-80%

- Insulation – Flat roof construction

This variable introduced seven different options for analysis. All the layers have remained the same, except for the thickness insulating layer, which was tested for multiple combinations:

Table 5.7 – Thickness options for the insulating layer of the flat roof

Flat Roof - Stone wool	
Thickness (mm)	Variation
100	0
120	+20%
140	+40%
180	+80%
80	-20%
60	-40%
20	-80%

- Insulation – Ground floor construction

This variable introduced seven different options for analysis. All the layers have remained the same, except for the thickness insulating layer, which was tested for multiple combinations:

Table 5.8 – Thickness options for the insulating layer of the ground floor

Ground floor - XPS	
Thickness (mm)	Variation
50	0
60	+20%
70	+40%
90	+80%
40	-20%
30	-40%
10	-80%

- Airtightness

The minimum value studied for airtightness was 0,60 ac/h, while the maximum was 4,00 degrees, with steps of 0,20 ac/h in between.

- Ventilation area

The minimum value studied for ventilation area was 0,00 m^2, while the maximum was 2,00 m^2, with steps of 0,50 m^2 in between.

- Thermal mass construction - window frames

This variable introduced six different options for analysis, such as:

1 – Aluminium window frame (no break);
2 – Aluminium window frame (with thermal break);
3 – Dummie (U=glass; other props=PVC frame);
4 – Painted wooded window frame;
5 – UPVC window frame;
6 – Wooden window frame.

- Infiltration

The minimum value studied for infiltration was 0,00 ac/h, while the maximum was 1,40 ac/h, with steps of 0,20 ac/h in between.

5.6.3 Results of the parametric analysis

The results of the parametric analysis are shown in Tables 5.9 to 5.11, for the Csa, Csb and Cfb climatic regions, respectively. The impact on performance is ranked according to the following classification on energy consumption variation (ECV):

$$ECV \geq 20\% \rightarrow \text{Very High}$$
$$20\% > ECV \geq 10\% \rightarrow \text{High}$$
$$10\% > ECV \geq 5\% \rightarrow \text{Medium}$$
$$5\% > ECV \geq 2{,}5\% \rightarrow \text{Low}$$
$$2{,}5\% > ECV > 0\% \rightarrow \text{Very Low}$$
$$ECV = 0 \wedge OTV = 0 \rightarrow \text{Null}$$

Table 5.9 – Results of the parametric analysis conducted on the Csa climate

Parametric Analysis - Csa			
Design Variables	Energy Consumption Variation	Operative Temperature Variation	Impact on Performance
Infiltration	31,81%	3,40%	Very High
Glazing Type	29,31%	3,55%	Very High
Insulation - External wall	11,15%	1,24%	High
Insulation - Flat roof	7,08%	0,69%	Medium
Building orientation	6,57%	1,28%	Medium
Thermal mass construction	3,79%	1,01%	Low
Window to wall %	1,95%	0,37%	Very Low
Local shading type	1,86%	1,24%	Very Low
Window blind type	1,49%	0,27%	Very Low
Airtightness	1,49%	0,14%	Very Low
Ventilation area	1,49%	0,14%	Very Low
Insulation - Ground floor	0,00%	0,00%	Null

Table 5.10 – Results of the parametric analysis conducted on the Csb climate

Parametric Analysis - Csb			
Design Variables	Energy Consumption Variation	Operative Temperature Variation	Impact on Performance
Glazing Type	33,26%	4,18%	Very High
Infiltration	29,71%	3,48%	Very High
Building orientation	12,90%	1,82%	High
Insulation - External wall	11,06%	1,32%	High
Insulation - Flat roof	7,55%	0,50%	Medium
Thermal mass construction	4,87%	0,96%	Low
Window to wall %	4,19%	0,73%	Low
Local shading type	3,35%	1,37%	Low
Airtightness	2,45%	0,23%	Very Low
Ventilation area	2,45%	0,23%	Very Low
Window blind type	2,35%	0,91%	Very Low
Insulation - Ground floor	0,00%	0,00%	Null

Table 5.11 – Results of the parametric analysis conducted on the Cfb climate

Parametric Analysis - Cfb			
Design Variables	Energy Consumption Variation	Operative Temperature Variation	Impact on Performance
Glazing Type	37,02%	4,52%	Very High
Infiltration	34,36%	3,73%	Very High
Insulation - External wall	12,91%	4,86%	High
Insulation - Flat roof	7,70%	0,74%	Medium
Thermal mass construction	6,11%	1,78%	Medium
Building orientation	4,82%	0,69%	Low
Local shading type	2,48%	1,09%	Very Low
Window to wall %	0,99%	0,30%	Very Low
Airtightness	0,57%	0,10%	Very Low
Window blind type	0,53%	0,94%	Very Low
Ventilation area	0,49%	0,10%	Very Low
Insulation - Ground floor	0,00%	0,00%	Null

In regards to the "Insulation – Ground floor" (Table 5.11), the results do not mean the parameter does not have any influence at all in terms of energy consumption and operative temperature, only the interval of results tested proved to be void. Furthermore, an additional higher range of thickness options were tested, which demonstrated to have small influence on the results.

5.7 Optimization settings

The structure of the optimization problem will determine the success of the test run and the adequacy of the solutions. Therefore, it is essential to select the elements that correctly characterize the case study. Design Builder's optimization tool allows for two objective functions, unlimited constraints and ten design variables.

5.7.1 Objectives

The main goal of this research is to optimize the energy efficiency of a lightweight steel building. Energy efficiency is defined by the International Energy Agency as "a way of managing and restraining the growth in energy consumption. Something is more energy

efficient if it delivers more services for the same energy input or the same services for less energy input" (http://www.iea.org/topics/energyefficiency/). Therefore, I will try to achieve the same or even better levels of building performance, in terms of comfort and lighting, with less energy demand from external sources. In order to display the aim of this problem, the following objective functions were chosen:
"Minimize Total Site Energy (kWh)" establishes the target of reducing the energy needs of the case study model. Total site energy compromises all the energy consumption of the building in the form of lighting, ventilation, cooling and heating. It represents the raw fuel billed by the energy company to the building.
"Minimize Discomfort ASHRAE 55 - all winter and summer clothes (h)" is the opposing target, indicating the need for lowering the unmet load hours.

5.7.2 Constraints

Buildings are one of the main sources of CO2 emissions and contributors to the degradation of the environment (Jones et al, 1998). So as to introduce a parameter of environmental sustainability to the problem, the operational CO2 emissions of the building should be limited. The CO2 emissions will be restricted to the recommended value for the use phase of the building of 68,50 kg/m^2*a (Nemry et al., 2008). Thus, the following constraint was added to the settings of the problem:
"Operational CO2 emissions less than 8562,50 kg".

For low energy buildings, the recommended airtightness rate is 0,60 ac/h (University of Exeter, Air Leakage Testing). The airtightness depends on a number of variables (ventilation, infiltration, exfiltration, wind direction, etc.). The mechanical ventilation system for all models was already established as 0,60 ach/h which is high; so the infiltration rate will not be restricted for the optimization analysis. By itself, the air infiltration to guarantee an airtightness rate of 0,60 ac/h would have to be 0,0042 ac/h (University of Exeter, Air Leakage Testing).

5.7.3 Variables

Based on the parametric analysis results, the selected design variables for the optimization problem consist of:

- Glazing type (Csa, Csb and Cfb);
- Infiltration(Csa, Csb and Cfb); ;
- Insulation – External wall construction (Csa, Csb and Cfb);
- Insulation – Flat roof construction (Csa, Csb and Cfb);
- Building orientation (Csa and Csb);
- Thermal mass construction - window frames (Cfb).

6 OPTIMIZATION ANALYSIS

6.1 Simulations

The simulation environment corresponds to the data space generated through an EnergyPlus annual simulation (1st of January to 31st of December) on which the optimization simulations will be performed. Thus, every output should be read as yearly values. DesignBuilder uses EnergyPlus format hourly weather data to reproduce external conditions for the building site, such as the external temperature, solar radiation and atmospheric conditions. These hourly weather data sets are data derived from hourly observations at a specific location by the national weather service.

The optimization tool for the 4.6.0.015 version of DesignBuilder does not upload automatically the optimization settings for the model, therefore new models have to be built, taking into account the optimization settings of each Pareto solution, to obtain the optimized results.

6.1.1 Optimization settings

The choice of the optimization settings affects the overall quality of the solutions, convergence and running time of the algorithm. Every optimization problem behaves differently and there is no standard configuration for the most efficient settings. According to De Jong (2002), basing the choice on settings that have been used to solve efficiently a similar optimization problem can guarantee reliability. Therefore, the initial settings were based on the results of the work of Aladjmi and Wright (2014), which studied a comparable energy efficiency problem and concluded that a population size of 5 and number of generations of 250 were the combination with the best performance. However, this premise will be assessed and experimentation with different combinations will take place before reaching a conclusion. Hence, five test runs on the same Csb model were performed (Table 6.1), consisting of varying the number of generations and population size in order to find the best performance of the algorithm. The remaining simulation parameters maintained the default definitions established on DesignBuilder.

Table 6.1 – Test runs performed on Model 1 (Csb climate)

Simulation	Number of generations	Population size
1	250	5
2	250	10
3	250	3
4	300	5
5	200	5

The first simulation for the Model 1 demonstrated a superior performance overall, which will be displayed on the following sections (6.1.3; 6.1.4; 6.2; 6.3). Consequently, the same settings were selected as the definitive combination to apply on simulations for the Csa and Cfb climates (Model 2 and 3, respectively) to achieve the best performance. The results for the Pareto front are illustrated in the Figures 6.1 to 6.7.

6.1.2 Optimization Results

The Pareto fronts for all the performed simulations are displayed on the following graphs:

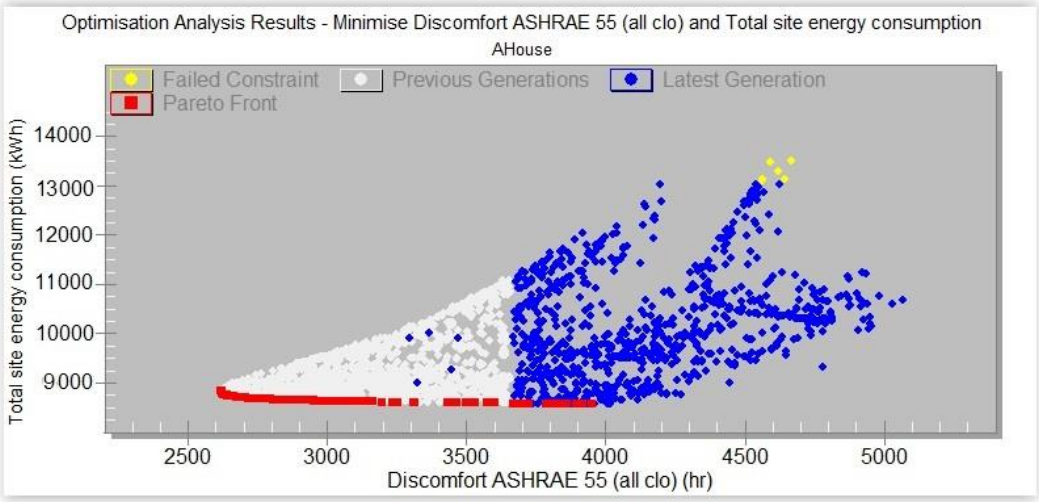

Figure 6.1 – Pareto front for the Simulation 1 (Csb)

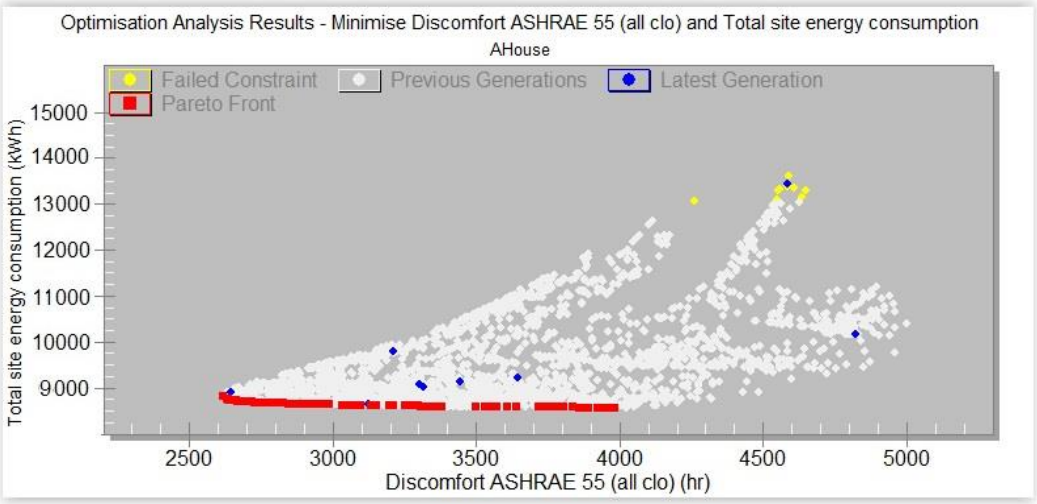

Figure 6.2 – Pareto front for the Simulation 2 (Csb)

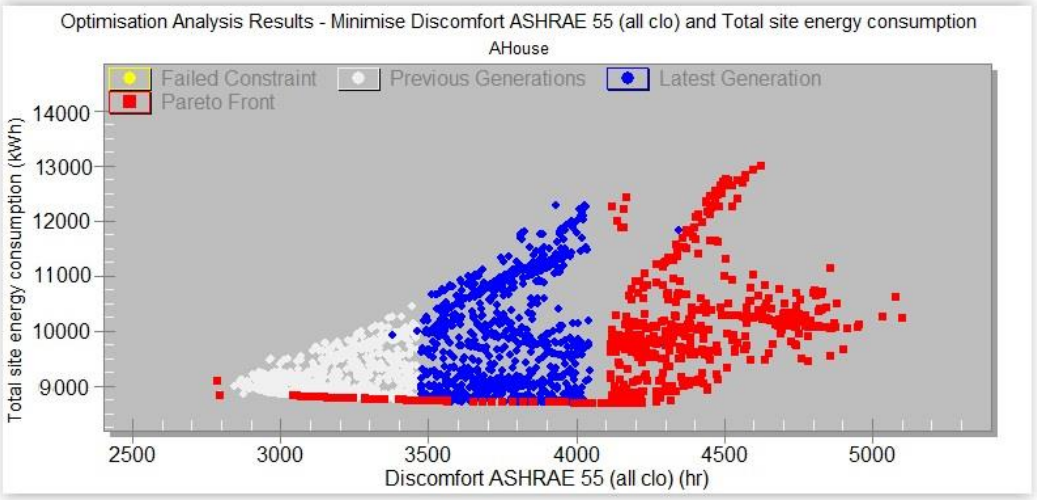

Figure 6.3 – Pareto front for the Simulation 3 (Csb) *

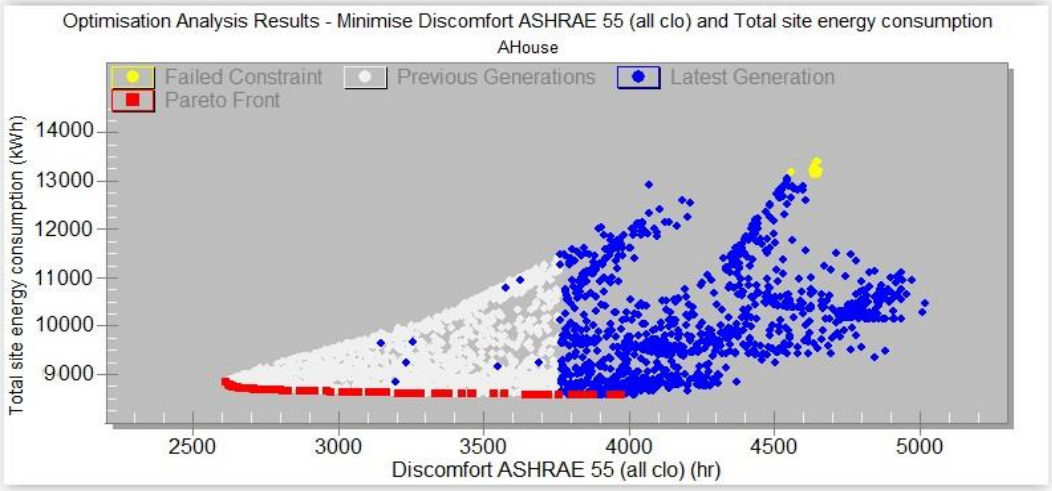

Figure 6.4 – Pareto front for the Simulation 4 (Csb)

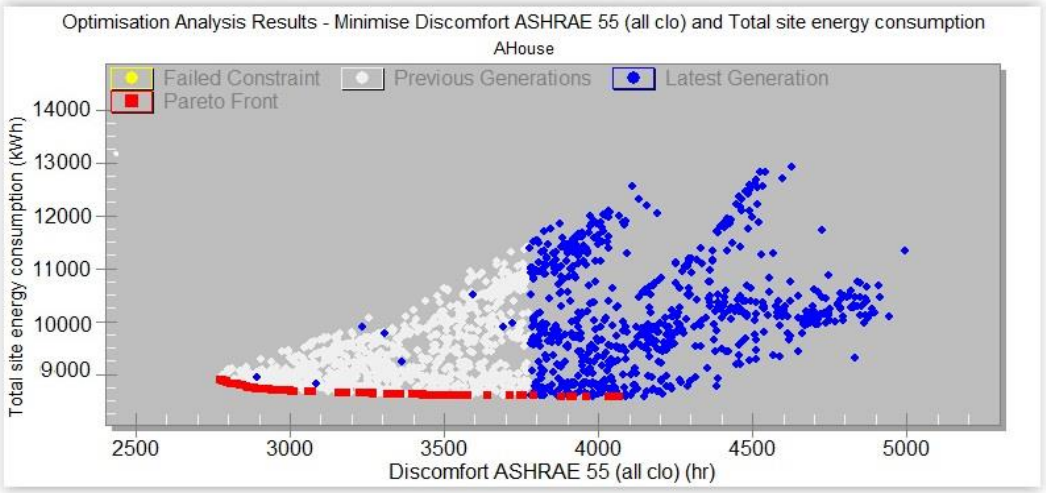

Figure 6.5 – Pareto front for the Simulation 5 (Csb)

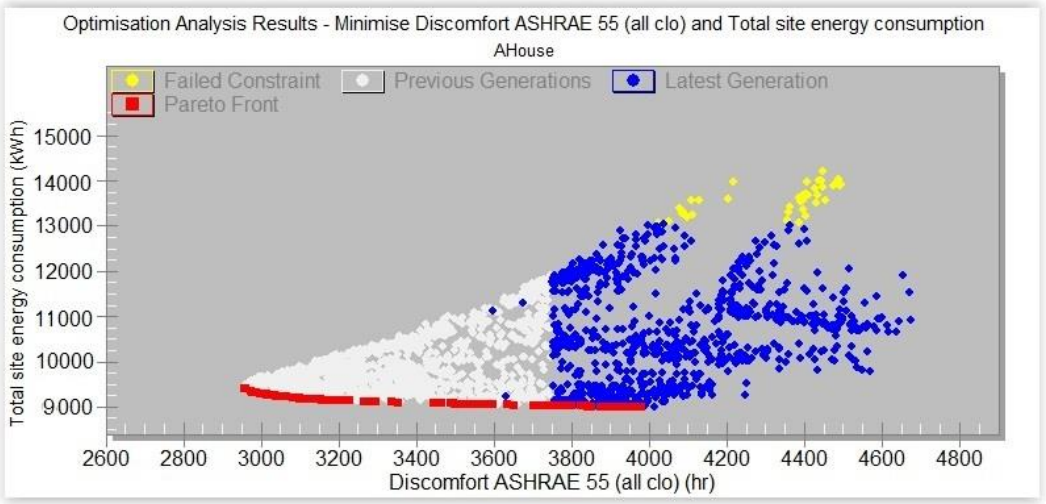

Figure 6.6 – Pareto front for the Simulation 6 (Csa)

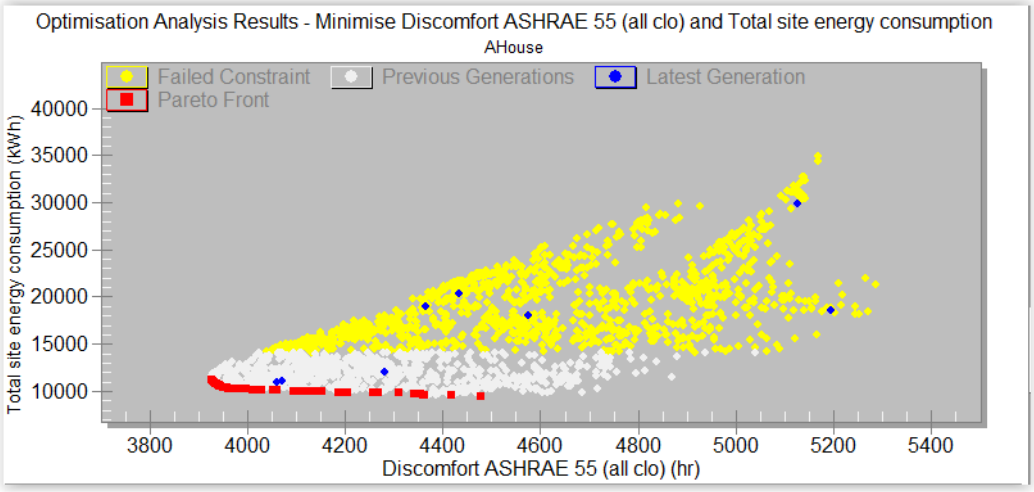

Figure 6.7 – Pareto front for the Simulation 7 (Cfb)

* It appears that some kind of bug happens when Simulation 3 is run on DesignBuilder and the graphical output confuses the latest generation data with Pareto front solutions. However, the numerical results are not compromised by the graphical error.

The evolution of the Pareto front in all the graphs is trending towards a full curve of optimal solutions, which is an indication of successful optimization. It is interesting to note that Simulation 5 never produced a failed constraint (Figure 6.5). As expected, more challenging environments, such as a humid climate (Figure 6.7), originate more failed constraints. Furthermore, to get a full picture of the comparison between the different climates, a juxtaposition of the Simulation 250 – 5 graphs is available in the Appendix (Figure A.4), along with the superposition of all the simulations for the Csb climate (Figure A.5).

6.1.3 Selection of Pareto solutions

Further testing will be conducted on the Pareto solutions which provoke the highest impact on the chosen objective functions, as the selection criteria. Therefore, the fourteen solutions that provided minimum values for each of the objective functions have been selected, since this is a minimization problem. In order to simplify the presentation of the results, only the table containing the results for the simulations with superior performance (250 – 5) will be featured in the main text, while the rest of the tables can be consulted in the Appendix section (Tables A. 10 to A.18).

Table 6.2 – Results for the objective functions (Pareto 1, 2, 11, 12, 13 and 14)

Post-Optimization results: Optimization analysis						
Optimized Features	Pareto 1	Pareto 2	Pareto 11	Pareto 12	Pareto 13	Pareto 14
Simulation	1	1	6	6	7	7
Climate	Csb	Csb	Csa	Csa	Cfb	Cfb
Number of generations	250	250	250	250	250	250
Population size	5	5	5	5	5	5
Minimization goal	Site Energy	Discomfort	Site Energy	Discomfort	Site Energy	Discomfort
Site energy (kWh)	8115,4	8453,24	9046,77	9865,32	10680,75	11467,48
Discomfort (h)	3948	2616	3983	2955	4751	4092

The results for the design variables of the corresponding Pareto solution are the following:

Table 6.3 – Results for the design variables (Pareto 1 - Csb)

Pareto 1	
Simulation	1
Climate	Csb
Glazing type	Vertical glazing, 0%-40% of wall, U-0.35 (1.99), SHGC-0.45
Infiltration (ac/h)	0,000
Insulation - External wall construction	LSF with 216 mm insulation thickness
Insulation - Flat roof construction	Roof with 180 mm insulation thickness
Building orientation (º)	44,18

Table 6.4 – Results for the design variables (Pareto 2 - Csb)

Pareto 2	
Simulation	1
Climate	Csb
Glazing type	Vertical glazing, 0%-40% of wall, U-0.35 (1.99), SHGC-0.45
Infiltration (ac/h)	0,233
Insulation - External wall construction	LSF with 216 mm insulation thickness
Insulation - Flat roof construction	Roof with 180 mm insulation thickness
Building orientation (º)	56,32

Table 6.5 – Results for the design variables (Pareto 11 - Csa)

Pareto 11	
Simulation	6
Climate	Csa
Glazing type	Vertical glazing, 0%-40% of wall, U-0.35 (1.99), SHGC-0.45
Infiltration (ac/h)	0,001
Insulation - External wall construction	LSF with 216 mm insulation thickness
Insulation - Flat roof construction	Roof with 180 mm insulation thickness
Building orientation (º)	22,60

Table 6.6 – Results for the design variables (Pareto 12 - Csa)

Pareto 12	
Simulation	6
Climate	Csa
Glazing type	Vertical glazing, 0%-40% of wall, U-0.35 (1.99), SHGC-0.45
Infiltration (ac/h)	0,215
Insulation - External wall construction	LSF with 216 mm insulation thickness
Insulation - Flat roof construction	Roof with 180 mm insulation thickness
Building orientation (º)	44,18

Table 6.7 – Results for the design variables (Pareto 13 - Cfb)

Pareto 13	
Simulation	7
Climate	Cfb
Glazing type	Vertical glazing, 0%-40% of wall, U-0.35 (1.99), SHGC-0.45
Infiltration (ac/h)	0,001
Insulation - External wall construction	LSF with 216 mm insulation thickness
Insulation - Flat roof construction	Roof with 180 mm insulation thickness
Thermal mass – window frame	Aluminium window frame (with thermal break)

Table 6.8 – Results for the design variables (Pareto 14 - Cfb)

Pareto 14	
Simulation	7
Climate	Cfb
Glazing type	Vertical glazing, 0%-40% of wall, U-0.35 (1.99), SHGC-0.45
Infiltration (ac/h)	0,156
Insulation - External wall construction	LSF with 216 mm insulation thickness
Insulation - Flat roof construction	Roof with 180 mm insulation thickness
Thermal mass – window frame	Wooden window frame

6.1.4 Quality of the output and running time

Computational effort is one of the benchmarks of an algorithm's performance. So as to test the efficiency of the simulations, the discrepancies in running time caused by using a different initial population size and number of generations were quantified. A timer was used to perform five trials for each iteration, aiming to eliminate human error. The average running time values are the following:

Table 6.9 – Running time analysis (Population size)

Running time analysis – Population size					
Iteration	Simulation 3 (250 - 3)	Variation	Simulation 1 (250 - 5)	Variation	Simulation 2 (250 - 10)
	Running Time (s)		Running Time (s)		Running Time (s)
1	68	+34,44%	104	+46,00%	192
2	69	+34,19%	105	+46,10%	194
3	68	+34,21%	104	+46,14%	192

Table 6.10 – Running time analysis (Number of generations)

Running time analysis - Number of generations					
Test run	Simulation 5 (200 - 5)	Variation	Simulation 1 (250 - 5)	Variation	Simulation 4 (300 - 5)
	Running Time (s)		Running Time (s)		Running Time (s)
1	20867	+20,00%	26083	+16,67%	31300

According to the Table 6.2, Table 6.9 and the Appendix section (Tables A.19 and A.21); it is clear that incrementing the initial population size does not necessarily guarantee a decrease in terms of "Total site energy":

- -0,03% when the population sizes is enhanced from 3 (8117,55 kWh) to 5 (8115,40 kWh) and the running time rises more than 34,00%;
- +0,14% when the population sizes is enhanced from 5 (8115,40 kWh) to 10 (8127,08 kWh) and the running time rises more than 46,00%.

By observing the Table 6.2, Table 6.9 and the Appendix section (Tables A.19 and A.21); it is possible to conclude that there is a decrease on the "Discomfort ASHRAE 55 (all clo)" output when the population size is incremented, but it is rapidly trending towards zero:

- -1,06% when the population sizes is enhanced from 3 (2644 h) to 5 (2616 h) and the running time rises more than 34,00%;
- -0,04% when the population sizes is enhanced from 5 (2616 h) to 10 (2615 h) and the running time rises more than 46,00%.

According to the Table 6.2, Table 6.10 and the Appendix section (Tables A.19 and A.21); it is possible to conclude that there is a decrease on the "Total site energy" output when the number of generations is incremented, but it is rapidly trending towards zero:

- -0,32% when the number of generations is enhanced from 200 (8141,70 kWh) to 250 (8115,40 kWh) and the running time rises 20,00%;
- -0,01% when the number of generations is enhanced from 250 (8115,40 kWh) to 250 (8114,66 kWh) and the running time rises 16,67%.

By observing the Table 6.2, Table 6.10 and the Appendix section (Tables A.19 and A.21); it is clear that incrementing the number of generations does not necessarily guarantee a decrease in terms of "Discomfort ASHRAE 55 (all clo)" hours:

- -0,08% when the number of generations is enhanced from 200 (2618 h) to 250 (2616 h) and the running time rises 20,00 %;

- +0,04% when the number of generations is enhanced from 250 (2616 h) to 300 (2617 h) and the running time rises 16,67%.

Therefore, Simulation 2 (250 – 10) and Simulation 4 (300 – 5) should be automatically excluded, since they originate inferior results along with longer running time. Simulation 1 (250 – 5) continuously generates superior results; however there is also a significant increase in running time. The user should be able to decide if the trade-off is worth it or not, according to the available time to run the analysis. Simulation 3 (250 – 3) provides satisfactory results and has the shortest running time. Simulation 5 (200 – 5) produces marginally better results than Simulation 3 (250 – 3), but has a markedly worse running time (+18,19%), so this simulation was rated as having a medium performance compared to all the test runs.

Overall, the deciding factor for this project is quality of the results and Simulation 1 (250 – 5) originated superior output for the two objective functions. Thus, Simulation 1 can be classified as the best performance for this specific problem.

6.2 Performance of the Pareto solutions

In this section, the behaviour of the fourteen Pareto solutions previously chosen will be evaluated, in order to demonstrate the discrepancies in terms of performance between different simulations for the same model and the disparity of results between the three climate zones. The performance criteria will be the following:

- "Annual total site energy consumption" (kWh)

This parameter is extracted from the ABUPS data after running an EnergyPlus annual simulation on the simulation models. It represents the raw fuel billed by the energy company to the building.

- "Annual fuel consumption" (kWh)

This parameter is extracted from the "Fuel totals" category after running an EnergyPlus annual simulation on the simulation models. It represents the converted fuel that is needed to assure the energy demands of the building are met, in terms of net values.

- "Annual operational CO2 emissions" (kg)

This parameter is extracted from the "CO2 production" category after running an EnergyPlus annual simulation on the simulation models. It represents the quantity of CO2 produced by the building during its operational stage.

- "Discomfort hours ASHRAE 55 - all winter and summer clothes" (h)
- "Average operative temperature for all summer" (ºC)
- "Average operative temperature for all winter" (ºC)
- "Heating degree hours" (h)
- "Cooling degree hours" (h)

6.2.1 Discussion of the results (Energy and environmental criteria)

The summary of the results can be found in the Appendix section (Tables A.19 to A.24). By observing the results, it is possible to conclude that major achievements were made regarding a decrease in energy consumption. For all the simulations done on the Csb model, the improvements in "Annual total site energy consumption" range from -40,16% to -43,37% (Table A.22). Pareto 7, 1 and 5 are the solutions with superior performance, in descending order. The improvements on the Csa model ranged from -42,54% to -47,31% (Table A.23). As expected, due to the regional weather conditions, the performance of the model located in the Cfb climate remains worse than the other two climates, but the impact on performance is greater in terms of percentage (-56,14% and -52,91%, according to Table A.24). The same premise also applies for the comparison between the Csb and Csa results.

The percentage change of the "Annual fuel consumption" and "Annual operational CO2 emissions" is exactly the same throughout the analysis, which proves a direct link between the energy and environmental performance of the building. The improvements made were also significant: -39,10% to -46,78% for the Csb climate; -41,95% to -48,84% for the Csa climate and -52,51% to -56,65% for the Cfb climate.

The figures for "Annual fuel consumption" also demonstrate that the optimized models were set up correctly, since the values match the optimization results for "Total site energy" calculated with a COP equal to 1.

6.2.2 Post-optimization comfort levels

The graphs demonstrating the yearly evolution of the operative temperature for each Pareto solution compared to the performance of the reference models are the following:

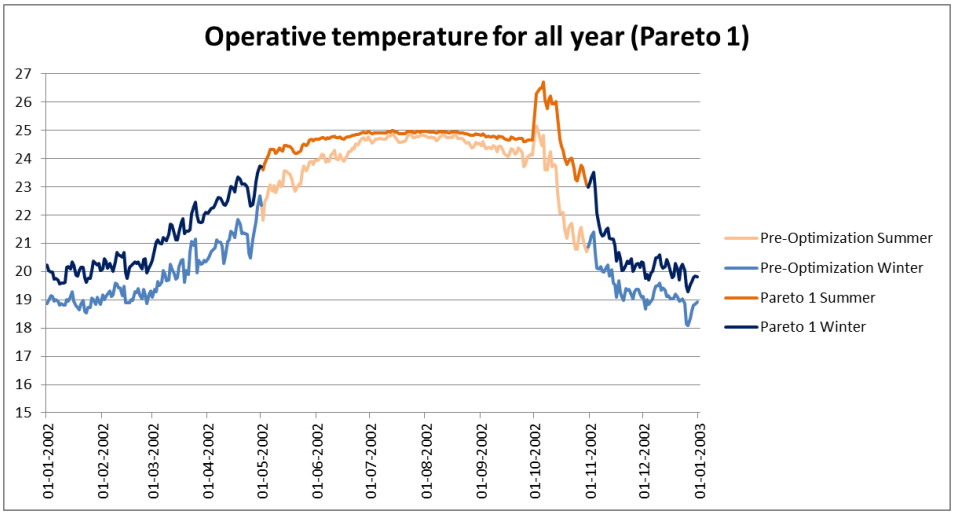

Figure 6.8 – Operative temperature for all year (Pareto 1 results for the Csb climate)

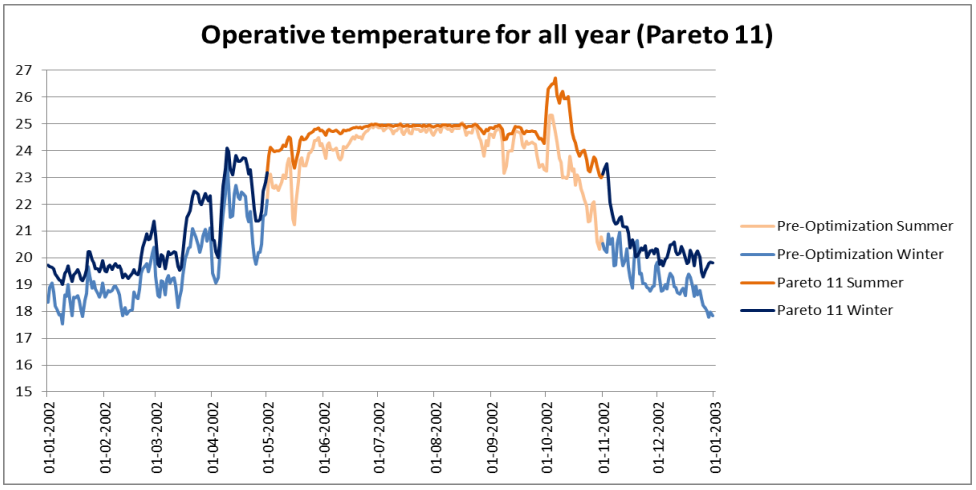

Figure 6.9 – Operative temperature for all year (Pareto 11 results for the Csa climate)

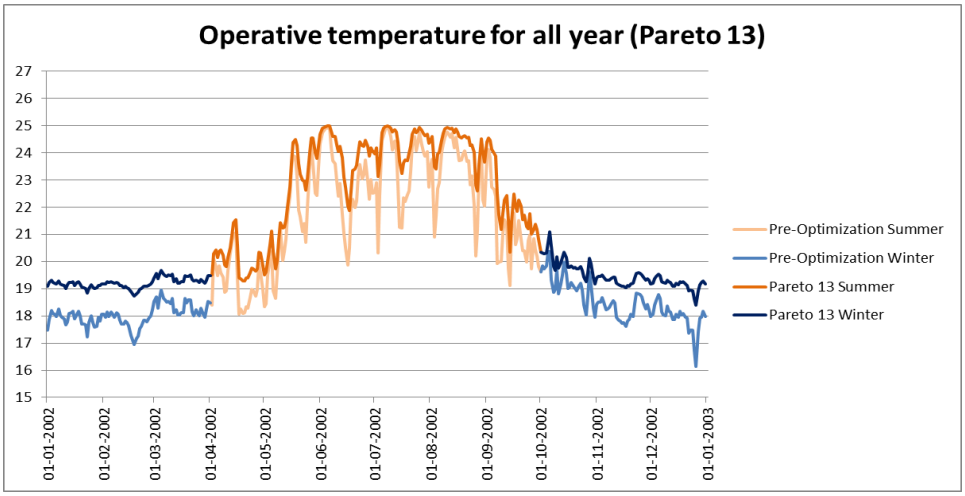

Figure 6.10 – Operative temperature for all year (Pareto 13 results for the Cfb climate)

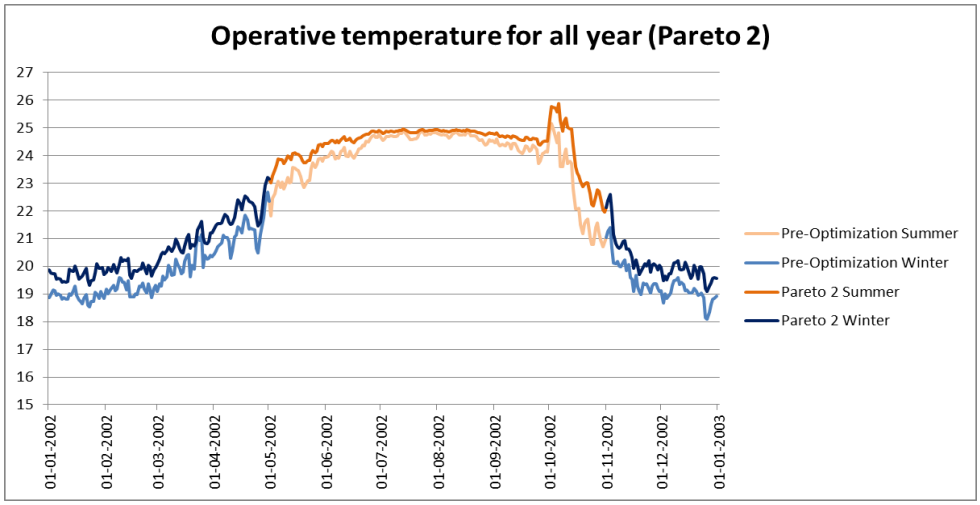

Figure 6.11 – Operative temperature for all year (Pareto 2 results for the Csb climate)

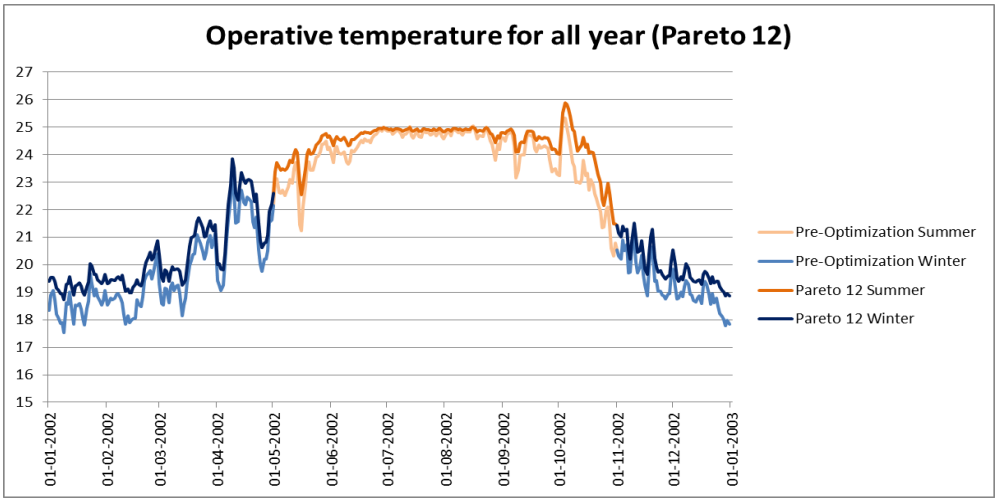

Figure 6.12 – Operative temperature for all year (Pareto 12 results for the Csa climate)

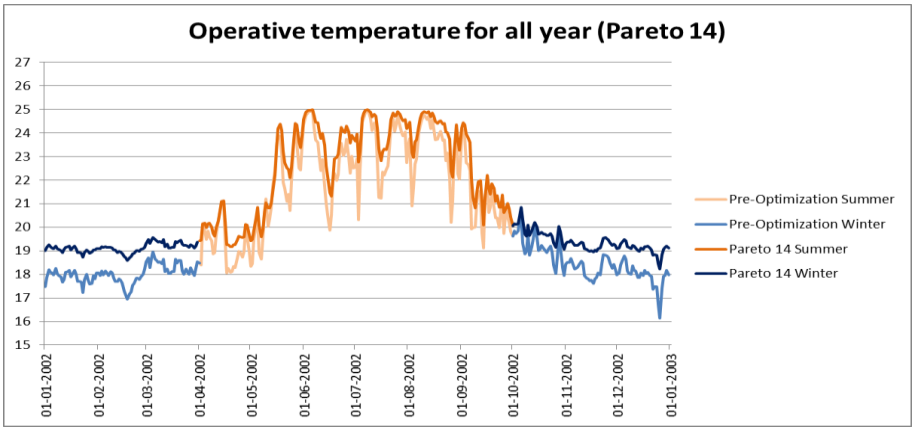

Figure 6.13 – Operative temperature for all year (Pareto 14 results for the Cfb climate)

The graphs demonstrating the weekly evolution of the operative temperature for each Pareto solution compared to the performance of the reference models are the following:

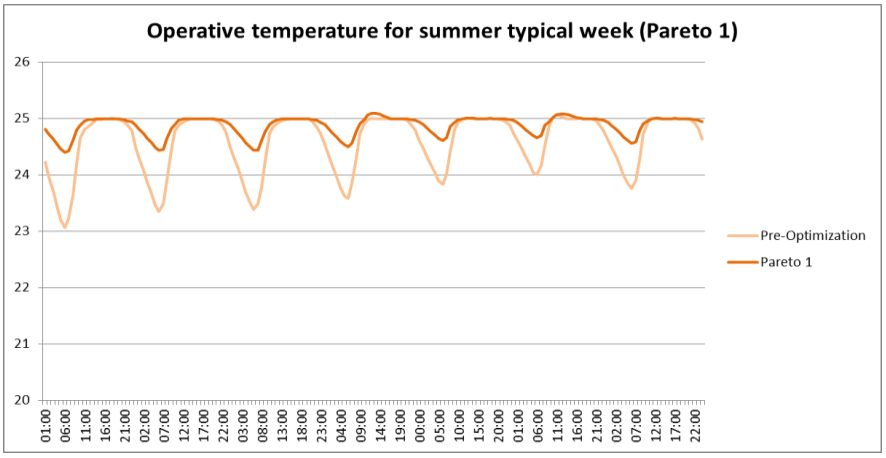

Figure 6.14 – Operative temperature for summer typical week (Pareto 1)

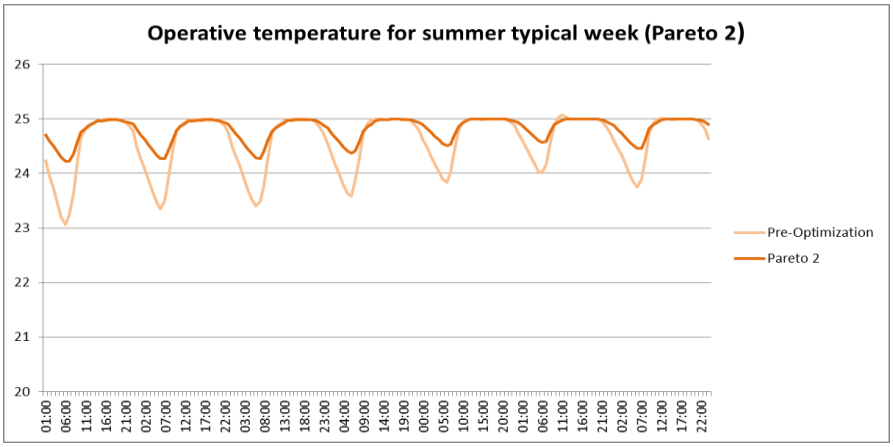

Figure 6.15 – Operative temperature for summer typical week (Pareto 2)

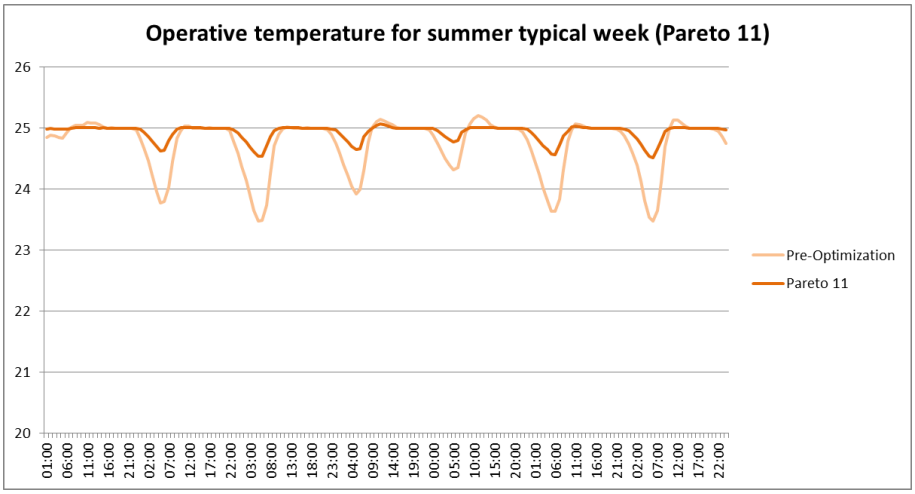

Figure 6.16 – Operative temperature for summer typical week (Pareto 11)

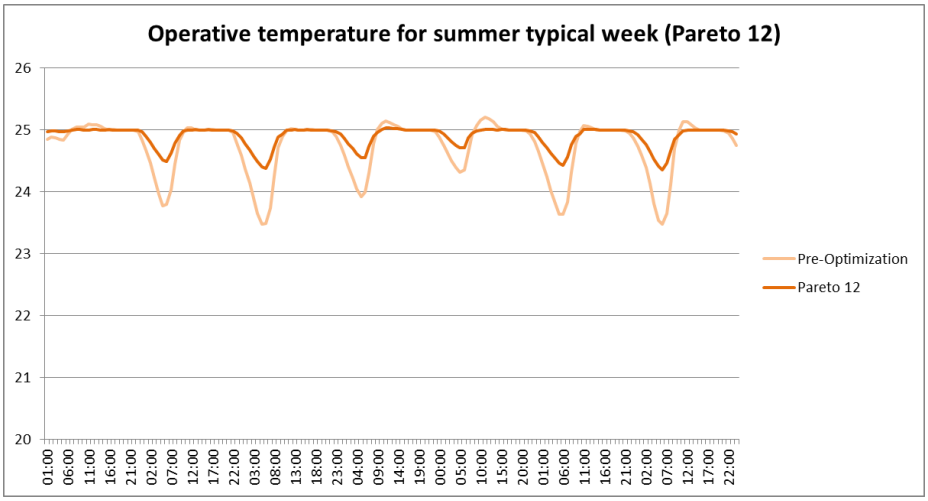

Figure 6.17 – Operative temperature for summer typical week (Pareto 12)

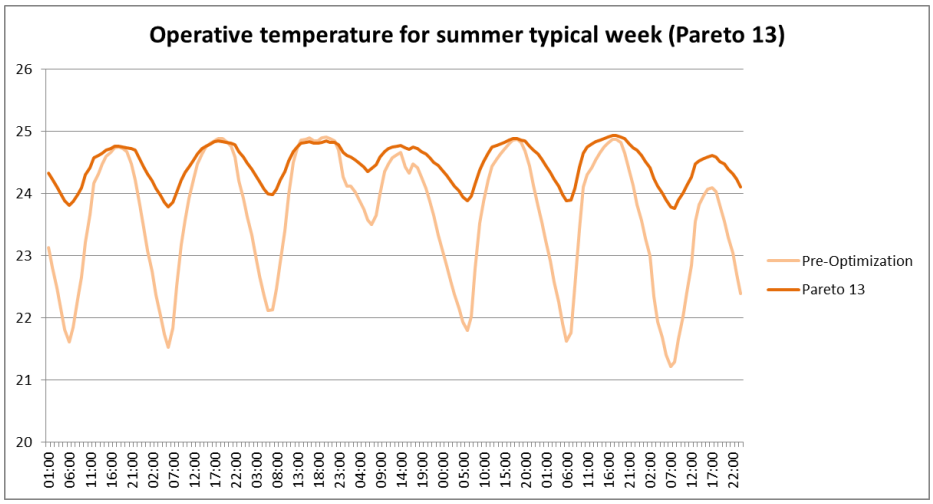

Figure 6.18 – Operative temperature for summer typical week (Pareto 13)

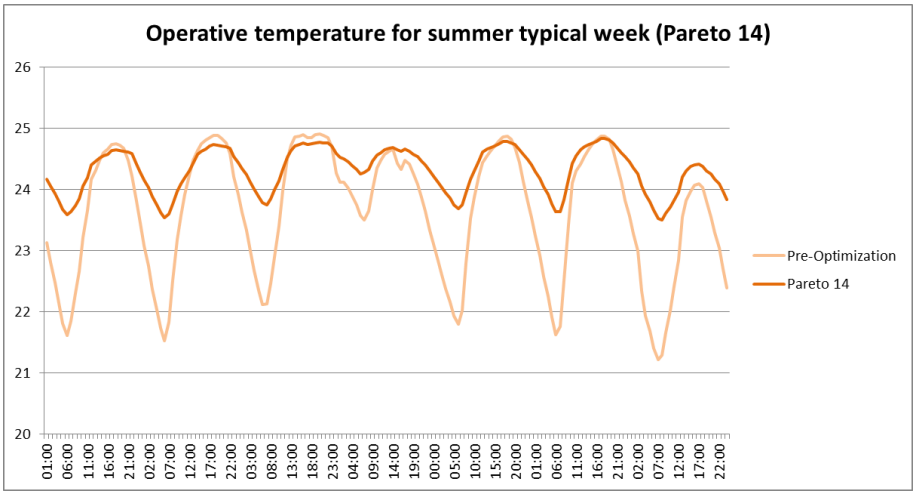

Figure 6.19 – Operative temperature for summer typical week (Pareto 14)

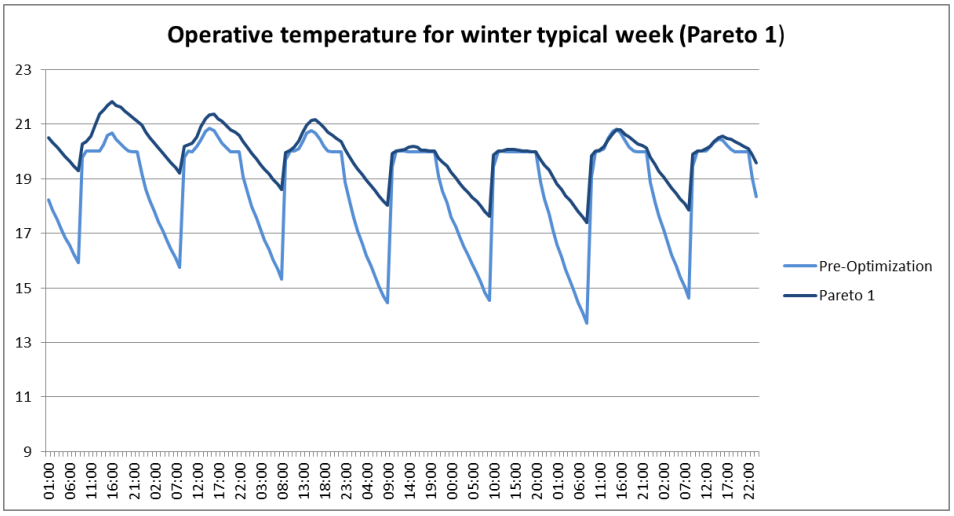

Figure 6.20 – Operative temperature for winter typical week (Pareto 1)

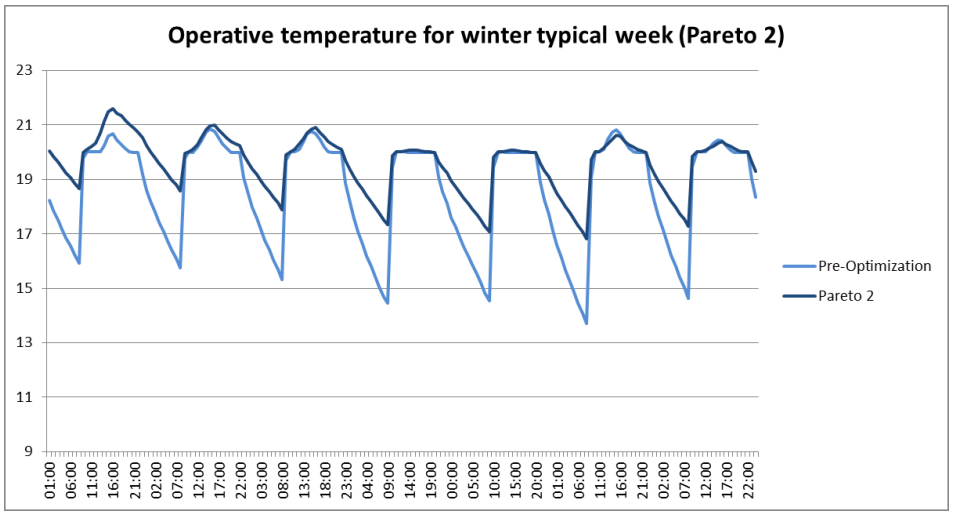

Figure 6.21 – Operative temperature for winter typical week (Pareto 2)

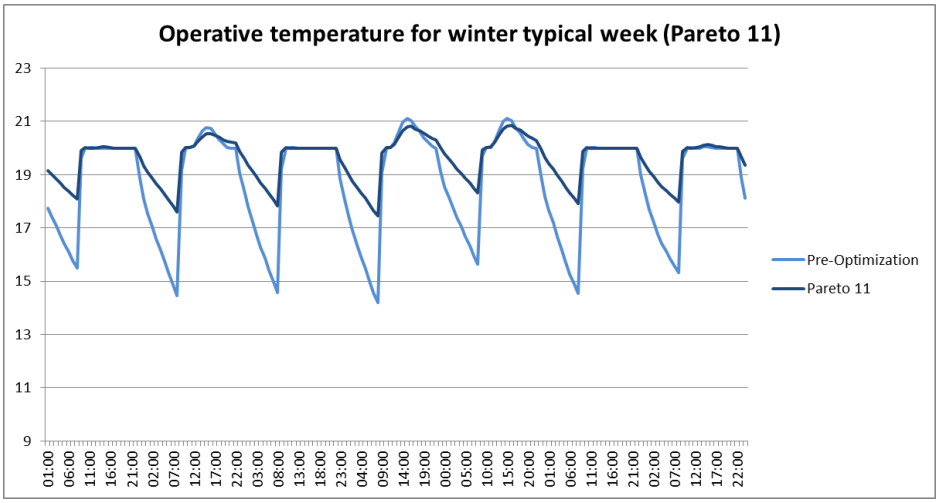

Figure 6.22 – Operative temperature for winter typical week (Pareto 11)

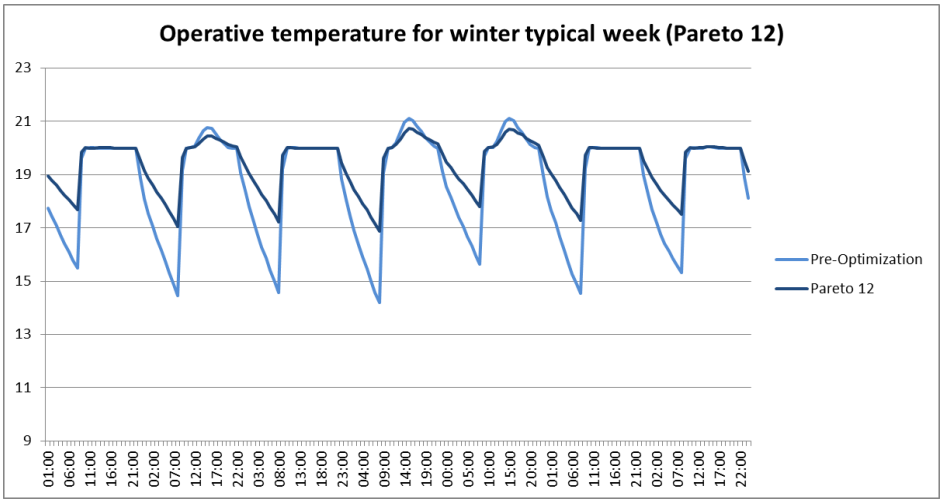

Figure 6.23 – Operative temperature for winter typical week (Pareto 12)

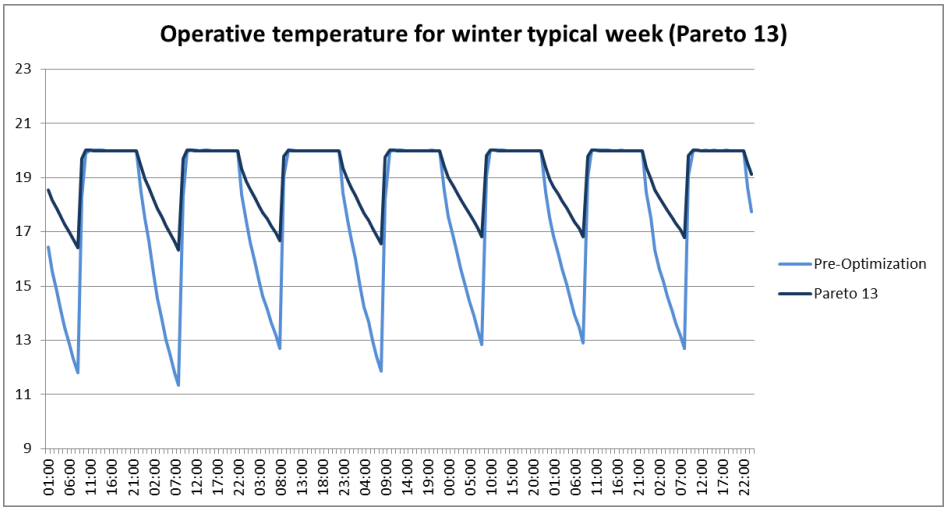

Figure 6.24 – Operative temperature for winter typical week (Pareto 13)

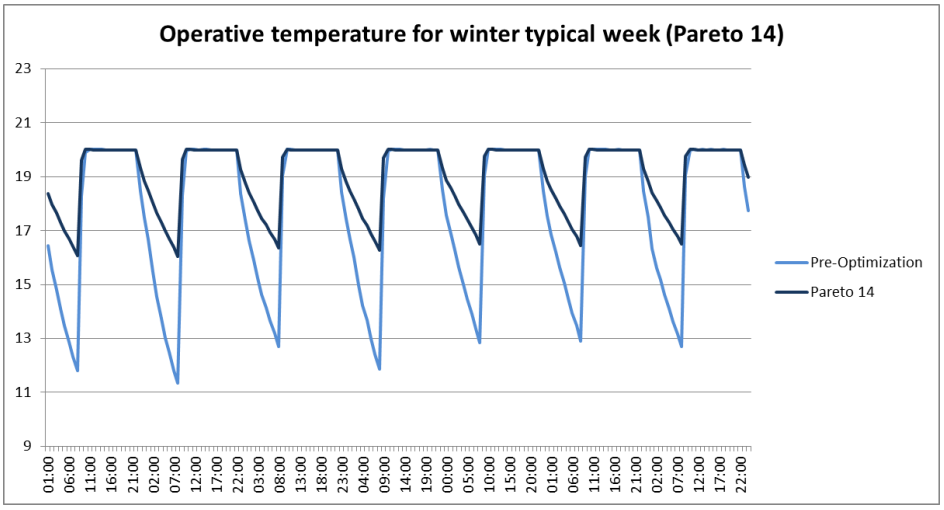

Figure 6.25 – Operative temperature for summer typical week (Pareto 14)

6.2.3 Discussion of the results (Thermal criteria)

For the even Pareto solutions, clear improvements were reached in terms of HDH for the Csb climate, ranging from -19,84% to -21,87% (Table A.22). The results for the Csa climate were also upgraded through a reduction of 10,73% (Table A.23). Nevertheless, the HDH for the Cfb climate only had a very slight reduction of -2,53% (Table A.24). Regarding CDH, the cuts ranged from -1,12% to -3,92% for the Csb climate (Table A.22); -7,62% for the Csa climate (Table A.23) and -0,88% for the Cfb climate (Table A.24). Pareto 10 marked an exception to the trend, since the CDH values increased slightly (+1,68%).

Ultimately, the Pareto solutions that aimed for the total minimization of "Discomfort ASHRAE 55 (all clo)" ended up generating positive outcomes, conciliating both the decrease of discomfort hours with the reduction of energy consumption. Hence, proving that it is in fact possible to improve the thermal conditions of the building and lower its energy dependency at the same time, without it being mutually exclusive. The decreases in overall discomfort hours ranged from -14,49% to -15,43% for the Csb climate; -9,88% for the Csa climate and -2,08% for the Cfb climate (Tables A.22 to A.24, respectively). The leading cause of the upgrade in comfort levels can be attributed to the decrease in heating demands.

On the contrary, for odd Pareto solutions, both the CDH and HDH significantly increased compared to the results of the reference models, with the exception of the HDH for the Cfb climate. The CDH results ranged from +58,70% to +59,48% for Csb climate (Table A.22); +34,70% for the Csa climate (Table A.23) and +96,69% for the Cfb climate (Table A.24). The HDH results ranged from +15,42% to +16,56% for Csb climate (Table A.22); +16,05% for the Csa climate (Table A.23) and -14,12% for the Cfb climate (Table A.24).

Conclusively, Pareto solutions akin to the strict minimization of "Total site energy (kWh)" performed badly in the thermal assessment, by worsening the comfort levels of the building. The increases in overall discomfort hours ranged from +27,68% to +28,59% for the Csb climate; +21,47% for the Csa climate and +13,69% for the Cfb climate (Tables A.22 to A.24, respectively). The leading cause of the downgrade in comfort levels can be attributed to the huge increase in cooling demands.

Furthermore, after the optimization, the average operative temperature for the "all summer" timeframe rose slightly, as well as average operative temperature for the "all winter" period (Tables A.19 to A.24 and Figures 6.8 to 6.13). The temperature increase was consistently higher for the odd Pareto solutions, as can be seen by comparing the Figures 6.14 to 6.25. One of the main benefits of the optimization procedure was the ability of diminishing the hourly fluctuations of temperature, to create a more stable environment inside the building.

6.2.4 Analysis of the trade-off between energy consumption and comfort levels

The trade-off between energy consumption and comfort levels of the building has been one of the central themes of this research. This concept can be evidenced by overlapping the graph corresponding to the yearly evolution of operative temperature with the total fuel consumption of the building.

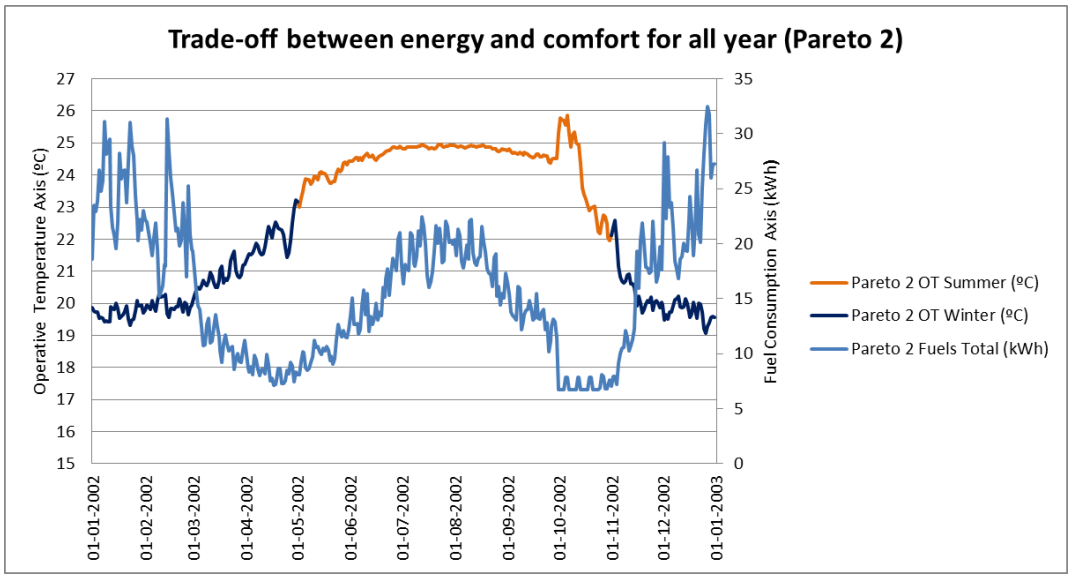

Figure 6.26 – Trade-off between energy and comfort for all year (Pareto 2)

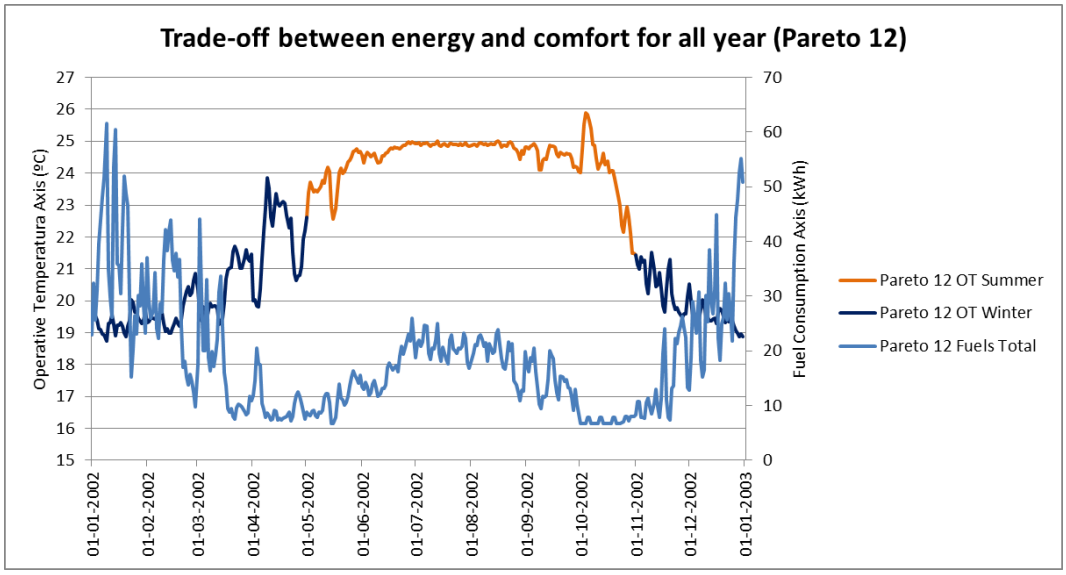

Figure 6.27 – Trade-off between energy and comfort for all year (Pareto 12)

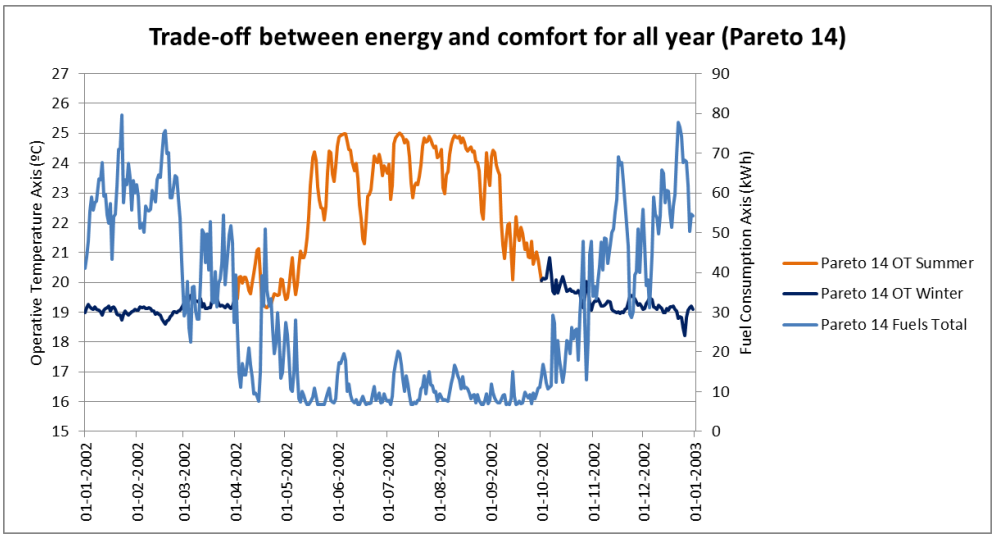

Figure 6.28 – Trade-off between energy and comfort for all year (Pareto 14)

The peaks of energy consumption occur within the coldest and warmest months of the year for the Csa and Csb climates (Figures 6.26 to 6.27), when the space condition needs are higher. For the Cfb climate, the days of warmest months of the year are generally still below the cooling setpoint, so cooling demands are less significant. The highest amounts of fuel consumption coincide with the winter months for all climates, matching the previous conclusion of the heating demands being the main cause of energy inefficiency of the building.

One flaw that needs to be addressed is the heat spell that crops up in the beginning of October for the Csb and Csa climates (Figures 6.26 and 6.27). The explanation lies on the fact that the cooling settings for HVAC are only turned on during the months corresponding to the "Summer (Northern Hemisphere)", as can be observed by the low fuel consumption during those days. This modeling option was due to the fact that DesignBuilder only allows the optimization analysis to take place during the year of 2002 and does not use average weather data, so the idea was to eliminate unnecessary energy consumption for days that presented abnormal temperature (such as a hot day in November). However, using the templates "Summer (Northern Hemisphere)" and "Winter (Northern Hemisphere)" proved to be slightly ineffective for these two climates, since there is a mismatch in the beginning of the October month, which should be included in the summer season due to higher temperatures.

The outside dry-bulb temperature is the temperature of air measured by a thermometer freely exposed to the air and shielded from radiation and moisture, thus being a good indicator of the outside air temperature. As can be observed in the figures below (Figure 6.29 and 6.30), the heat peaks in October happen after periods of increase of outside air temperature close to summer temperatures for the Csb and Csa climates. Due to the design features of the building (very low infiltration and thick insulation), the heat accumulates indoors. In order to tackle this issue and perfect the comfort levels of the building to the detriment of keeping the energy consumption lower, the solution would be to create a new schedule template that would extend the summer season to include the month of October for the Csb and Csa climates.

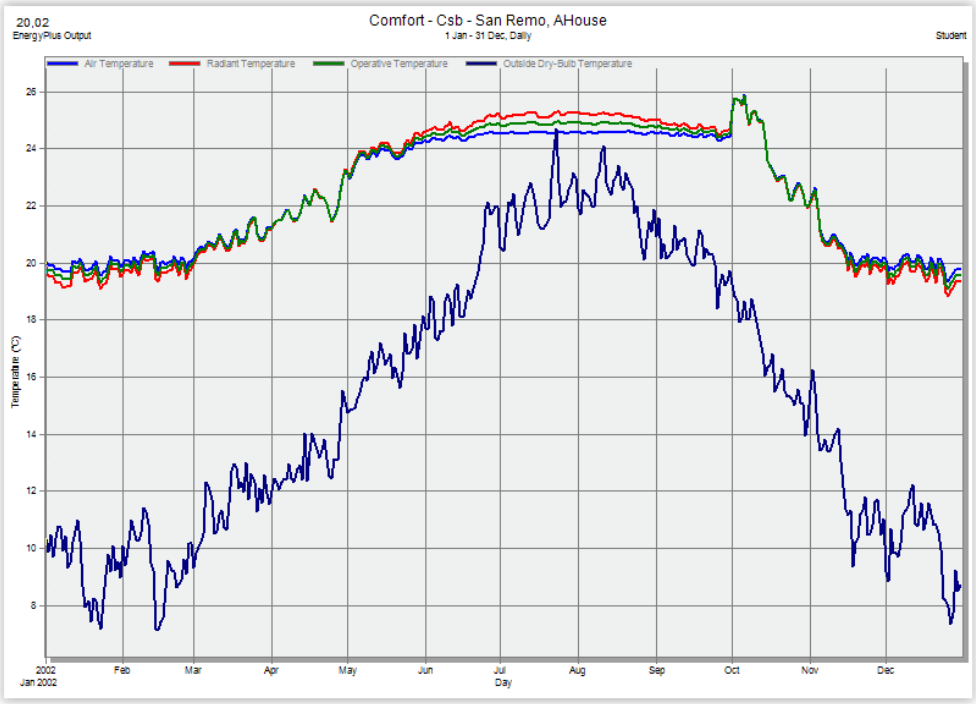

Figure 6.29 – Compilation of temperature data for all year (Pareto 2)

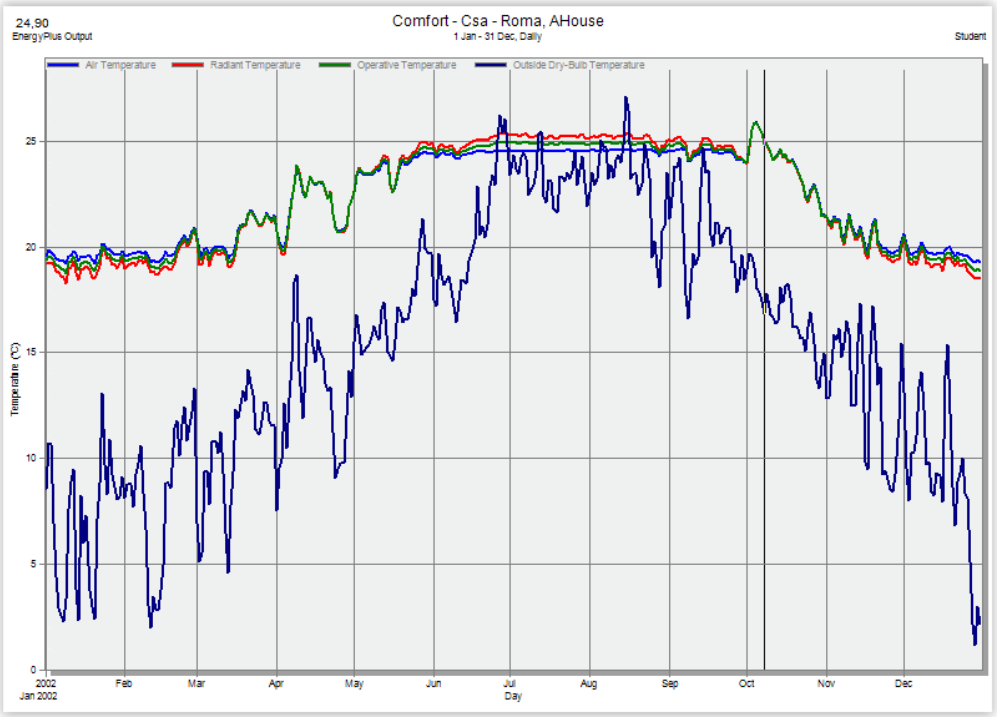

Figure 6.30 – Compilation of temperature data for all year (Pareto 12)

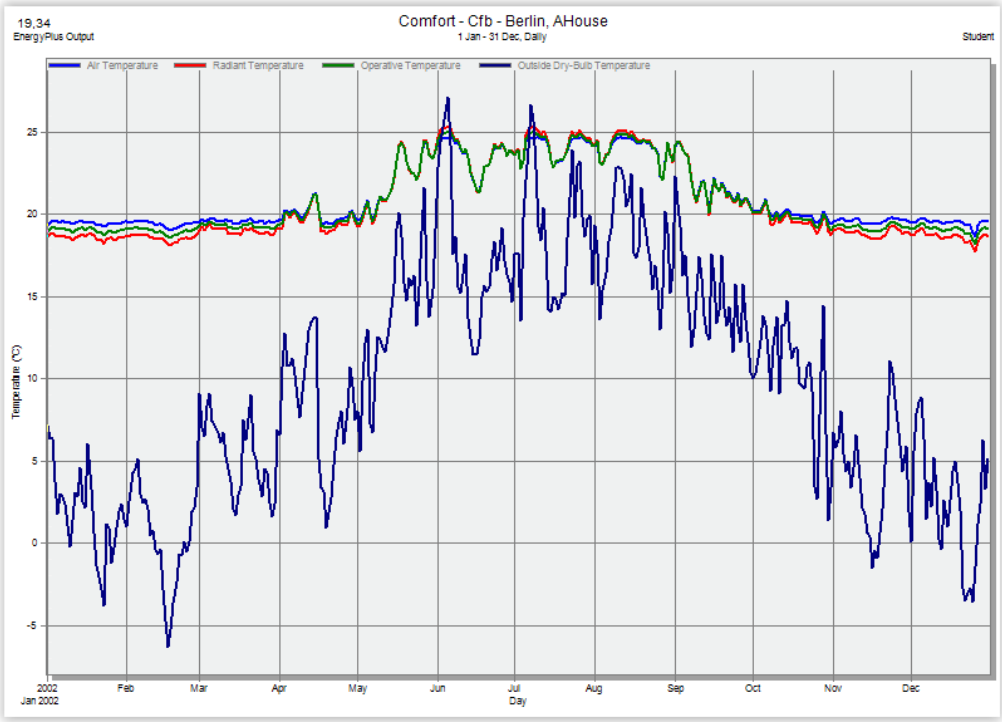

Figure 6.31 – Compilation of temperature data for all year (Pareto 14)

6.3 Statistical analysis of the Pareto set

In order to study the convergence and the evolution over time of the Pareto optimal solutions, two complementary analyses were conducted: optimal design distribution and characterization of the type solutions for each climate.

6.3.1 Optimal design distribution

The optimal design distribution consists of sorting the Pareto solutions according to the iterations where they were first generated. This distribution will provide insight of the strength of the simulation (the more solutions generated, the stronger the simulation will be).

The distribution results for the Simulations 1, 6 and 7 are the following:

Table 6.11 – Optimal design distribution for the Simulation 1

Optimal design distribution - Optimization analysis						
Generation	Csb		Csa		Cfb	
	Simulation 1 (250 - 5)	Distribution 1	Simulation 6 (250 - 5)	Distribution 6	Simulation 7 (250 - 5)	Distribution 7
0-50	1	0,93%	1	1,11%	2	2,22%
51-100	24	22,43%	13	14,44%	12	13,33%
101-150	30	28,04%	24	26,67%	12	13,33%
151-200	27	25,23%	31	34,44%	13	14,44%
201-250	25	23,36%	39	43,33%	23	25,56%
251 - 300	-	-	-	-	-	-
Total	107	100,00%	108	100,00%	62	100,00%

The complete results for all the simulations can be found in the Appendix section (Table A.25 and A.26).

By comparing all the tables for the Csb climate, Simulation 1 (250 – 5) exhibits the superior performance regarding the quantity of optimal solutions. It is interesting to note that using a higher initial population size or number of generations does not correlate with producing a greater amount of optimal solutions. For the Simulation 1, the generation of optimal solution has peaked during the middle of the simulation and is trending towards being unable to produce as many optimal solutions, which indicates convergence of solutions. According to the Table 6.11, the Csb and the Csa climate originate almost as many optimal solutions, while the Cfb climate creates considerably less Pareto solutions. This is expected, since the Cfb climate provides harsher weather conditions, which constrains the optimization analysis.

6.3.2 Type solutions

The aim of typifying the Pareto set is to provide a clear picture of the most statistically common design options that produce good energy performance. Additionally, there is a visible pattern of design choices by the end of the simulation, which can be considered an indicator of convergence of the solutions.

The tables containing the results for the simulations with superior performance (250 – 5) can be found in the Appendix section (Tables A.27 to A.29).

Type solution for the Csb climate (Table A.27):

The optimal solutions share the same glazing type, insulation thickness for external wall construction and flat roof construction for 100% of the instances. The maximum values for infiltration and building orientation are 0,233 ac/h and $70,82^0$, respectively. The minimum values for infiltration and building orientation are 0,000 ac/h and $39,46^0$. It is possible to conclude that the 55^0 to 65^0 range for building orientation is the most prolific in terms of generating optimal solutions, while the 0,050 ac/h to 0,100 ac/h interval produces greater output for infiltration.

Type solution for the Csa climate (Table A.28):

The optimal solutions share the same glazing type, insulation thickness for external wall construction and flat roof construction for 100% of the instances. The maximum values for infiltration and building orientation are 0,215 ac/h and $50,59^0$, respectively. The minimum values for infiltration and building orientation are 0,001 ac/h and $13,83^0$. It is possible to conclude that the 45^0 to 50^0 range for building orientation is the most prolific in terms of generating optimal solutions, while values below 0,05 ac/h produce greater output for infiltration.

Type solution for the Cfb climate (Table A.29):

The optimal solutions share the same glazing type, insulation thickness for external wall construction and flat roof construction for 100% of the instances. Aluminum window frame (with thermal break) is present on 75,81% of the Pareto solutions. The maximum value for infiltration is 0,178 ac/h and the minimum value is 0,001 ac/h. It is possible to conclude that the 55^0 to 65^0 range for infiltration is the most prolific in terms of generating optimal solutions.

6.4 Financial analysis of the Pareto set

One of the premises of this thesis is that replacing low energy performance with high energy performance is beneficial all around, even on a financial perspective. In this final section, the impact of choosing the optimal design options in terms of capital costs and operational costs of the building will be compared to the expenses of the original models.

6.4.1 Capital costs

Capital costs can be defined as "fixed, one-time expenses incurred on the purchase of land, buildings, construction and equipment (…)" (Center for International Environmental Law, http://www.ciel.org/Publications/climatechangeglossary.pdf). In this context, capital costs represent the expenses related to the cost of construction materials and equipment used for the building. The cost of changing the building orientation, infiltration and labor resources are too complex to estimate properly, so the term of capital costs will only refer from now on to the costs associated with glazing, insulation and window frames. The cost of the materials was assessed using information provided by DesignBuilder (glazing and window frames) and suppliers (insulation) for the year 2014. The analysis will be centered on the rise of expenses associated with upgrading the building.

The complete results for all the simulations are displayed on Tables 6.12 and 6.13. The Pareto solutions for the Csb and Csa climates were coupled due to generating the same expenses.

6.4.2 Operational costs

Operational costs can be defined as "the annual cost incurred on a continuous process" (Business Dictionary), such as maintaining the full operation of a building. In this case, I will resume the operational costs as the annual energy expenditure of the building in terms of lighting, heating, cooling and domestic hot water, which can be extracted from the "Total site energy" category on DesignBuilder. It is safe to assume that rest of the parameters that constitute the operational costs will remain the same whether the building has low or high energy performance, so it is fine to exclude them from the analysis. All these items exclusively use electricity as a fuel. In order to estimate the annual operating costs, a research was conducted on the household prices for electricity in Italy (0,234 €/kWh) and Germany (0,297 €/kWh) (Eurostat, 2015). These 2014 prices will rise throughout the years due to inflation, however, the same will happen for both the high and low energy performance, so the comparison will not be hurt by assuming static values for both of them.

The complete results for all the simulations are displayed on Tables 6.14 to 6.16.

6.4.3 Discussion of the results (Financial criteria)

By observing the capital costs results (Tables A.30 and A.31), it is possible to conclude that the increase in initial investment was generally low for all the Pareto solutions (1.112,79 €), except for the Pareto 13 solution (4.443,51 €). Overall, the models located in the Csa and Csb climates suffered a 12,26% increase in capital costs; while the Pareto 13 and Pareto 14 solutions (Cfb climate) originated 36,91% and 9,24%, respectively. The higher cost of the Pareto 13 solution is caused by the cost of the aluminium window frames (with thermal break), which are significantly more expensive than their wood counterparts.

In terms of operational costs (Tables A.32 to A.34), the decrease in expenses was extremely significant, ranging from -39,10% and -46,76% for the Csb climate; -48,84% and -41,95% for the Csa climate and -56,65% and -52,51% for the Cfb climate. These results are the same as the decreases met in "Annual Fuels Total", as expected.

Ultimately, the increase in capital costs to upgrade the building for optimal performance ends up being quickly compensated by the decrease in operational costs. In the best case scenario (Pareto 11), it would take 10 months for the home owner to equalize the initial investment and 14 months in the worst case scenario (Pareto 13). These timeframes were achieved by dividing the balance in capital costs between the reference and optimized models and the balance in yearly operational costs between the reference and optimized models.

Table 6.12 – Capital Cost Analysis for the Csb and Csa Climate

Capital Cost Analysis for the Csb and Csa Climate							
Material			Area (m2)	Price (€/m2)	Cost (€)	Capital Cost (€)	Variation (%)
Models	Reference	Simple window with 6 mm thickness - No glazing	50,20	-	6.444,53 €	9.074,52 €	-
		Clear glass with 3mm thickness - No glazing	7,50	-	965,29 €		
		LSF with 120 mm insulation thickness	200,90	5,79	1.163,21 €		
		Roof with 100 mm insulation thickness	100,70	4,98	501,49 €		
	Pareto	Vertical glazing, 0%-40% of wall, U-0.35 (1.99), SHGC-0.45	57,50	-	7.409,82 €	10.187,32 €	12,26%
		LSF with 216 mm insulation thickness	200,90	9,70	1.948,73 €		
		Roof with 180 mm insulation thickness	100,70	8,23	828,76 €		

Table 6.13 – Capital Cost Analysis for the Cfb Climate

Capital Cost Analysis for the Cfb Climate							
Material			Area (m2)	Price (€/m2)	Cost (€)	Capital Cost (€)	Variaton
Models	Reference	Simple window with 6 mm thickness - No glazing	50,20	-	6.444,53 €	12.040,30 €	-
		Clear glass with 3mm thickness - No glazing	7,50	-	965,29 €		
		LSF with 120 mm insulation thickness	200,90	5,79 €	1.163,21 €		
		Roof with 100 mm insulation thickness	100,70	4,98 €	501,49 €		
		Painted wooded window frame	57,70	51,40 €	2.965,78 €		
	Pareto 13	Vertical glazing, 0%-40% of wall, U-0.35 (1.99), SHGC-0.45	57,70	-	7.409,82 €	16.483,82 €	36,91%
		AH PrE1Perfis - Parede Exterior_1Ref 216 mm	200,90	9,70 €	1.948,73 €		
		Roof with 180 mm insulation thickness	100,70	8,23 €	828,76 €		
		Aluminium window frame (with thermal break)	57,70	152,92 €	8.823,20 €		
	Pareto 14	Vertical glazing, 0%-40% of wall, U-0.35 (1.99), SHGC-0.45	57,50	-	7.409,82 €	13.153,10 €	9,24%
		AH PrE1Perfis - Parede Exterior_1Ref 216 mm	200,90	9,70	1.948,73 €		
		Roof with 180 mm insulation thickness	100,70	8,23	828,76 €		
		Wooden window frame	57,70	51,40 €	2.965,78 €		

Table 6.14 – Operational Cost Analysis for the Csb Climate

Operational Cost Analysis for the Csb Climate											
Fuel Breakdown (kWh/year)	Pre-Optimization	Post-Optimization									
	Model 1	Simulation 1		Simulation 2		Simulation 3		Simulation 4		Simulation 5	
	Initial solution	E (250-5)	D (250-5)	E(250-10)	D(250-10)	E(300-5)	D(300-5)	E(250-3)	D(250-3)	E(200-5)	D(200-5)
		Pareto 1	Pareto 2	Pareto 3	Pareto 4	Pareto 5	Pareto 6	Pareto 7	Pareto 8	Pareto 9	Pareto 10
Lighting	2256,47	2256,47	2256,47	2256,47	2256,47	2256,47	2256,47	2256,47	2256,47	2256,47	2256,47
Heating	4898,08	1170,11	1845,28	1163,31	1793,05	1164,89	1817,33	1165,25	2031,99	1169,10	1735,56
Cooling	2154,66	1377,49	1272,07	1383,26	1280,11	1378,89	1269,34	1379,68	1251,82	1386,02	1288,58
DWH	330,42	330,42	330,42	330,42	330,42	330,42	330,42	330,42	330,42	330,42	330,42
Total	9639,63	5134,49	5704,24	5133,47	5660,05	5130,67	5673,56	5131,82	5870,70	5142,01	5611,03
Operational cost (€/year)	2.255,67 €	1.201,47 €	1.334,79 €	1.201,23 €	1.324,45 €	1.200,58 €	1.327,61 €	1.200,85 €	1.373,74 €	1.203,23 €	1.312,98 €
Variation in Operational cost	-	-46,74%	-40,83%	-46,75%	-41,28%	-46,78%	-41,14%	-46,76%	-39,10%	-46,66%	-41,79%

Table 6.15 – Operational Cost Analysis for the Csa Climate

Operational Cost Analysis for the Csa Climate			
Fuel Breakdown (kWh/year)	Pre-Optimization	Post-Optimization	
	Model 2	Simulation 6	
	Initial solution	E (250-5)	D (250-5)
		Pareto 11	Pareto 12
Lighting	2256,47	2256,47	2256,47
Heating	6607,28	1985,48	2786,90
Cooling	2507,56	1413,74	1419,09
DWH	330,42	330,42	330,42
Total	11701,72	5986,10	6792,88
Operational cost (€/year)	2.738,20 €	1.400,75 €	1.589,53 €
Variation in Operational cost	-	-48,84%	-41,95%

Table 6.16 – Operational Cost Analysis for the Cfb Climate

Operational Cost Analysis for the Cfb Climate			
Fuel Breakdown (kWh/year)	Pre-Optimization	Post-Optimization	
	Model 3	Simulation 7	
	Initial solution	E (250-5)	D (250-5)
		Pareto 13	Pareto 14
Lighting	2256,47	2256,47	2256,47
Heating	19366,03	6861,63	7872,33
Cooling	765,79	400,56	330,57
DWH	330,42	330,42	330,42
Total	22718,71	9849,08	10789,79
Operational cost (€/year)	6.747,46 €	2.925,18 €	3.204,57 €
Variation in Operational cost	-	-56,65%	-52,51%

7 CONCLUSIONS

Overall, the research objectives listed in the first chapter of this thesis were accomplished. The optimized building designs recommended for each climatic region have lower energy consumption, better comfort levels and are cheaper in the long run for the home owner. These key findings will be outlined in the following paragraphs. In the end of this chapter, recommendations for further improvements of the work are provided.

7.1 Summary of the key findings

The design variables with more impact in terms of energy performance are the same for the Csa and Csb climates ("Glazing type", "Infiltration", "Insulation – External Wall Construction", "Insulation – Flat Roof Construction" and "Building Orientation"); while "Thermal mass construction – window frames" replaces "Building orientation" for the Cfb climate.

Optimization settings consisting of 250 as the number of generations and 5 as the initial population size attain the ideal performance for this specific problem. This proposition is based on the superior results achieved, strong simulation in terms of generation of solutions (statistical evidence), the formation of a clear optimization curve (graphical evidence) and the demonstration of convergence.

Significant improvements were made for all the climates in terms of energy consumption, translated by the contraction in "Annual total site energy consumption" (ranging from 40,16% to 56,14%) and "Annual fuel consumption" (ranging from 39,10% to 56,65%). The direct link between energy and environmental performance of the building was proven throughout the analysis, since the percentage change was exactly the same for "Annual fuel consumption" and "Annual operational CO2 emissions.

The comfort levels analysis revealed the decrease in discomfort hours occurred alongside the reduction of energy consumption for the Pareto solutions which aimed for the minimization of the objective function "Discomfort ASHRAE 55 - all winter and summer clothes (h)". On the other hand, the Pareto solutions strictly promoting the minimization of "Total Site Energy (kWh) caused major deterioration of the comfort levels of the building, with slight gains in energy consumption reduction, compared to the even Pareto solutions (a small difference of

approximately 2,36% for the Csb climate; 4,77% for the Csa climate and 3,23% for the Cfb climate). Altogether, it is recommended to prioritize the Pareto solution correspondent to the global minimum for "Discomfort ASHRAE 55 - all winter and summer clothes (h)" for this problem, with the intention of creating a project with a well-rounded performance.

Several design characteristics were identified as forming a pattern of optimal solutions, therefore it is possible to frame type solutions to be followed by the designer that guarantee a good performance for all the climates.

The reduction of energy dependency is the most rational financial decision, since the massive decrease in operational costs outweighs the increase in capital costs (glazing, insulation and window frames) for the building in a matter of one year and two months in the most disadvantageous scenario for all climates.

7.2 Future works

Considerable progress will be achieved in the next years regarding the use of optimization tools during the design stage of the construction process. Technology that combines modeling with optimization algorithms is now accessible outside research environments and will be widely employed by companies that want to sell efficient products, which is a growing trend in the construction market (McGraw-Hill Construction, 2010).

In terms of future research, it would be advisable to conduct an expansion of this analysis when the optimization tools improve. Due to the early use of this technology, there were several issues related to the software not being able to handle heavier simulations and crashing. Despite the software being able to run up to ten design variables in theory, it was not able to perform simulations with more than five design variables without crashing. So as to improve the range of the analysis, it would be important to assess design combinations that encompass more variables.

In order to pursue the ideal simulation settings for this specific problem, different combinations of population size and number of generations were studied, since they were singled out by Alajmi and Wright (Alajmi and Wright, 2014) as having the most influence on the results of a similar energy efficiency problem. However, it would be pertinent to test this conclusion and verify if it also applies to this problem. Therefore, it would be recommended to study multiple combinations of mutation rate, crossover and tournament size, instead of using the default values for DesignBuilder.

The comfort levels for the Csb and Csa climates can be more refined by creating a new schedule template that would extend the summer season to include the month of October and

replacing the “Summer (Northern Hemisphere)” schedule template for HVAC; thus eliminating the heat spell. The number of discomfort hours would diminish and the energy consumption would be expected to rise, in terms of change of results compared to this solution.

The financial analysis conducted by the end of the thesis encountered several limitations in terms of cost estimation and ended up being very simplified. Thus, it would be advisable to add a cost estimation of the “Infiltration” and “Building Orientation” design variables to get the full picture of the fluctuations in investment.

REFERENCES

Alajmi, A. and Wright, J. (2014). “Selecting the most efficient genetic algorithm sets in solving unconstrained building optimization problem”. International Journal of Sustainable Built Environment, Volume 3, Issue 1.

Arnfield, J. A. (2016). “Köppen climate classification”, Encyclopaedia Britannica (http://www.britannica.com/science/Koppen-climate-classification).

ASHRAE (2014) “ASHRAE Handbook-Fundamentals”. American Society of Heating, Refrigerating and Air-Conditioning Engineers, Atlanta.

ASHRAE (2010) “Indoor Air Quality Guide: Best Practices for Design, Construction and Commissioning”. American Society of Heating, Refrigerating and Air-Conditioning Engineers, Atlanta.

ASHRAE Standard 55 (2013). "Thermal Environmental Conditions for Human Occupancy". American Society of Heating, Refrigerating and Air-Conditioning Engineers, Atlanta.

Athienitis, A. and Charron, R. (2006). “Design and Optimization of Net Zero Energy Solar Homes”. ASHRAE Transactions, Volume 112, Issue 2.

Baker, N. and Steemers, K. (2000) “Energy and Environment in Architecture: A Technical Design Guide”. E&FN Spon, London.

Bichou, Y. and Krarti, M. (2011). “Optimization of envelope and HVAC systems selection for residential buildings”. Energy and Buildings, Volume 43, Issue 12.

Boduch, M. and Fincher, W. (2009). “Standards of Human Comfort: Relative and Absolute”. University of Texas, School of Architecture, Meadows Seminar. (https://soa.utexas.edu/sites/default/disk/preliminary/preliminary/1-Boduch_Fincher-Standards_of_Human_Comfort.pdf)

Business Dictionary. (http://www.businessdictionary.com/definition/operating-cost.html)

Button, D. and Pye, B. (eds.) (1993) "Glass in building: Guide to modern architectural glass performance". Oxford: Butterworth Architecture.

Caldas, L. and Norford, L. (2003). "Genetic Algorithms for Optimization of Building Envelopes and the Design and Control of HVAC Systems". Journal of Solar Energy Engineering, Volume 125, Issue 3.

Center for International Environmental Law. "Climate Change Glossary". (http://www.ciel.org/Publications/climatechangeglossary.pdf)

Chiras, D. (2002). "The Solar House: Passive Heating and Cooling". Chelsea Green Publishing Company.

Coley, D. and Schukat, S. (2002). "Low-energy design: combining computer-based optimisation and human judgement". Building and Environment, Volume 37, Issue 12.

Danielski, I. et al (2012). "Adaption of the passive house concept in northern Sweden - a case study of performance". Conference paper (http://miun.diva-portal.org/smash/record.jsf?pid=diva2%3A685906&dswid=7037) presented at Passivhus Norden 2013, Gottemburg, Sweden, 15-17 October 2013.

Deb, K. et al (2002). "A Fast and Elitist Multiobjective Genetic Algorithm: NSGA-II". IEE Transactions on Evolutionary Computation, Volume 6, Issue 2.

European Directive 2002/91/EC. Directive 2002/91/EC of the European Parliament and of the Council of 16 December 2002 on the energy performance of buildings. Brussels, Belgium: Official Journal of the European Communities.

Energystar.gov. "Electric Tankless Water Heating: Competetive Assessment". (https://www.energystar.gov/ia/partners/prod_development/new_specs/downloads/water_heaters/ElectricTanklessCompetitiveAssessment.pdf)

European Directive 2010/31/EU. Directive 2010/31/EU of the European Parliament and of the Council of 19 May 2010 on the energy performance of buildings. Brussels, Belgium: Official Journal of the European Communities.

European Directive 2012/27/EU. Directive 2012/27/EU of the European Parliament and of the Council of 25 October 2012 on energy efficiency. Brussels, Belgium: Official Journal of the European Communities.

Eurostat, Statistics Explained (2015). "Half-yearly electricity and gas prices, second half of year, 2012–14 (EUR per kWh)". (http://ec.europa.eu/eurostat/statistics-explained/index.php/File:Half-yearly_electricity_and_gas_prices,_second_half_of_year,_2012%E2%80%9314_(EUR_per_kWh)_YB15.png)

Gonçalves, H. et al (1998). "Passive Solar Buildings in Portugal. Experiences in the Last 20 years". Department of Renewable Energies – INETI. Lisbon, Portugal.

Hastings, R. et al (2007). "Sustainable solar housing. Exemplary buildings and technologies". London: Earthscan, 2007. Vol.2, IEA task 28.

Horikoshi, K. et al (2012). "Building Shape Optimization for Sustainable Building Design-part (1) investigation into the relationship among building shape, zoning plans, and building energy consumption". Conference paper presented at Proceedings of ASim2012, the 1st Asia Conference of International Building Performance Simulation Association, Shanghai, China, 25-27 November 2012. (http://www.ibpsa.org/proceedings/asim2012/0125.pdf)

Jones, P.D. et al (1998) "High-resolution palaeoclimatic records for the last millennium: interpretation, integration and comparison with General Circulation Model control-run temperatures". The Holocene 8,4; pages 473–479.

Lawson, R.M. (2009) "Sustainability of Steel in Housing and Residential Buildings". The Steel Construction Institute, SCI Publication P370.

Mardookhy, M. (2013). "Energy Efficiency in Residential Buildings in Knoxville, TN, U.S". Master's Thesis, University of Tennessee, Tennessee.

McGraw-Hill Construction (2010). "Green BIM: How Building Information Modeling is Contributing to Green Design and Construction". SmartMarket Report, Beford, Massachussets.

McKnight, T. and Hess, D. (2000). "McKnight's Physical Geography: A Landscape Appreciation". Prentice Hall, Eleventh Edition, New Jersey.

Mitchell, M. (1996). "An Introduction To Genetic Algorithms". Bradford Book The MIT Press, Fifth Edition, Cambridge, Massachusetts.

Mitsubishi Electric. “Residential: Zuba Central”. (http://www.mitsubishielectric.ca/en/hvac/zuba-central/powerful_savings.html)

National Institute of Building Sciences. “Whole Building Design Guide”. (http://www.wbdg.org/)

Nemry, F. et al (2008) “Environmental Improvement of Potentials of Residential Buildings (IMPRO-Building)”. European Communities, 2009, Luxembourg.

Olgay, V. (1963). “ Design with Climate: Bioclimatic Approach to Architectural Regionalism”, Princeton University Press, 2016 Edition, Princeton.
Openeering. “Multiobjective optimization and Genetic algorithms”, (http://www.openeering.com/scilab_tutorials).

Pacheco, R. et al (2012). “Energy efficient design of building: A review”. Renewable and Sustainable Energy Reviews, Volume 16, pages 3559-3573.

Pedrosa, A. (2009). “Certificação Energética em Edifícios de Habitação Existentes: Caso de Estudo no Concelho de Leiria”. Master's Thesis, Universidade de Trás-os-Montes e Alto Douro, Vila Real, Portugal.

Pezeshk, S. et al (2002). “State of the Art on the Use of Genetic Algorithms in Design of Steel Structures”. Recent Advances in Optimal Structural Design, Edited by Scott A. Burns, ASCE Publications, 2002 Edition.

Pires, J. (2013). “O método prescritivo na construção de moradias em aço leve”. Master's Thesis, Instituto Superior Técnico, Lisbon, Portugal.

Powerknot. “How Efficient is Your Air Conditioning System?”. (http://www.powerknot.com/how-efficient-is-your-air-conditioning-system.html)

Rajeev, S. and Krishnamoorthy, C.S. (1992). “Discrete Optimization of Structures Using Genetic Algorithms”. ASCE Journal of Structural Engineering, Volume 118, Issue 5.

RCCTE. (2006). “Regulamento das Características de Comportamento Térmico dos Edifícios”. Decreto-Lei 80/2006, de 4 de Abril, Diário da República.

Roosa, S. A. (2010). “Sustainable Development Handbook”. Fairmont Press, 2008 Edition, Lilburn, Georgia.

Shi, X. (2011). “Design optimization of insulation usage and space conditioning load using energy simulation and genetic algorithm”. Energy, Volume 36, Issue 3.

Srinivas, N. and Deb, K. (1994). “Multiobjective optimization using Non-dominated Sorting in Genetic Algoritms”. Evolutionary Computation, Volume 2, Issue 3.

Talbi, E. (1965). “Metaheuristics: from design to implementation”. John Wiley & Sons, Inc., 2009 Edition, New Jersey.

Tuhus-Dubrow, D. and Krarti, M. (2010). “Genetic-algorithm based approach to optimize building envelope design for residential buildings”. Building and Environment, Volume 45, Issue 7.

Wang et al (2005). “Applying multi-objective genetic algorithmsin green building design optimization”. Building and Environment, Volume 40, pages 1512-1525.

Wright, J. et al (2002). “Optimization of building thermal design and control by multi-criterion genetic algorithm”. Energy and Buildings, Volume 34, Issue 9.

Yi, Y. K. and Malkawi, A. M. (2009). “Optimizing building form for energy performance based on hierarchical geometry relation”. Automation in Construction, Volume 18, Issue 6.

UNEP (2007). “Buildings and climate change – status, challenges and opportunities”. Paris, France: United Nations Environmental Programme.

University of Exeter. “Air Leakage Testing”. (http://www.exeter.ac.uk/media/universityofexeter/research/newsandevents/newsandeventsarchive/Air_Leakage_Testing.pdf)

US Air Force (2001). “Passive solar design handbook. Volume 1: Passive solar design concepts”. (https://www.wbdg.org/ccb/AF/AFH/pshbk_v1.pdf)

US Department of Energy (2008). “Energy Efficiency Trends in Residential and Commercial Buildings”. (http://apps1.eere.energy.gov/buildings/publications/pdfs/corporate/bt_stateindustry.pdf.).

USC Department of Architecture. Thermal guide (http://www.usc.edu/dept-00/dept/architecture/mbs/tools/thermal/shadedevice.html)

APPENDIX

Appendix I – Architectural plans

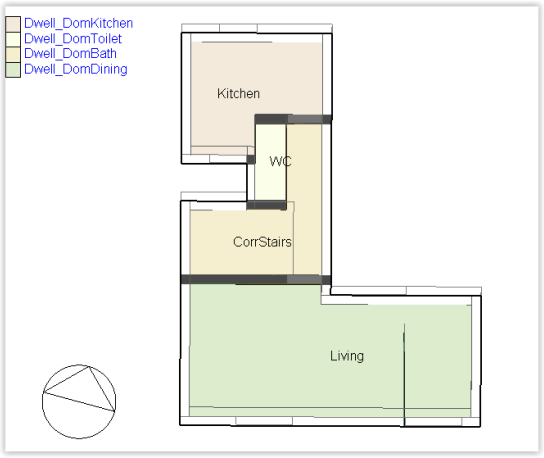

Figure A.1 – First floor plan

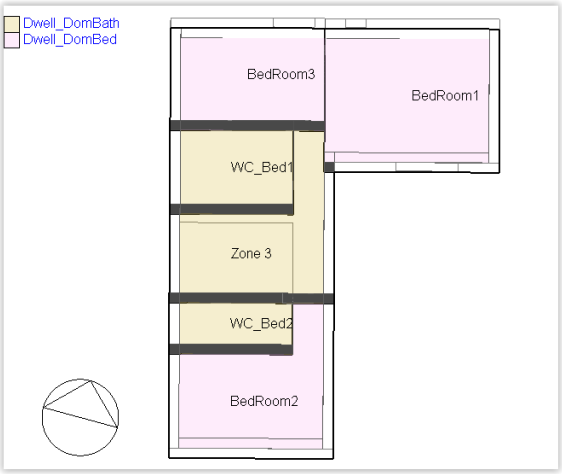

Figure A.2 – Second floor plan

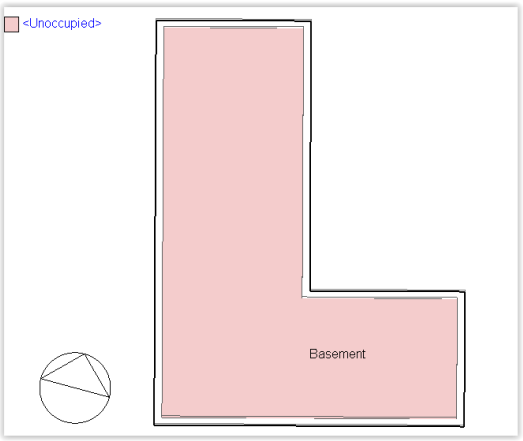

Figure A.3 – Basement plan

Appendix II – Elements of the model

Table A.1 – External wall of the original models

External wall		
Layer	Material	Thickness (mm)
1 (Outermost)	Reboco Acrílico Resinado	3
2	EPS cor (Standard)	40
3	Oriented stand board (OBS)	13
4	Air gap	25
5	MW Stone Wool (rools)	120
6 (Innermost)	Gypsum Plasterboard	15

Table A.2 – Flat roof of the original models

Flat roof		
Layer	Material	Thickness (mm)
1 (Outermost)	Copy of Mortar	30
2	XPS Extruded Polystyrene - CO2 Blowing	30
3	Air gap	30
4	Cast concrete (Lightweight)	40
5	Oriented stand board (OBS)	18
6	Air gap	25
7	MW Stone Wool (rools)	100
8 (Innermost)	Gypsum Plasterboard	15

Table A.3 – Ground floor of the original models

Ground floor		
Layer	Material	Thickness (mm)
1 (Outermost)	XPS Extruded Polystyrene - CO2 Blowing	50
2	Concrete, cast-aerated	180
3	Floor/Roof screed	13
4 (Innermost)	Ceramic/porcelain	100

Table A.4 – External floor of the original models

External floor		
Layer	Material	Thickness (mm)
1 (Outermost)	Reboco Acrílico Resinado	3
2	EPS cor (Standard)	30,9
3	Gypsum Plasterboard	15
4	Rock wool - unbonded	100
5	Air gap	25
6	Oriented stand board (OBS)	18
7	Floor/Roof screed	13
8 (Innermost)	Ceramic/clay tiles - ceramic tiles dry	10

Table A.5 – Internal floor of the original models

Internal floor		
Layer	Material	Thickness (mm)
1 (Outermost)	Gypsum Plasterboard	15
2	Rock wool - unbonded	4
3	Air gap	160
4	Oriented stand board (OBS)	18
5	Cement/plaster/mortar - cement creed	13
6 (Innermost)	Ceramic/clay tiles - ceramic tiles dry	10

Table A.6 – External windows of the original models

External Windows Pre-Optimization	
Glazing Type	Generic Clear 6 mm Glass
Total Solar Transmission (SHGC)	0,828
Light Transmission	0,881
Direct Solar Transmission	0,790
U-Value (ISSO 15099/NFRC) (W/m2-K)	5,801

Table A.7 – Internal windows of the original models

Internal Windows Pre-Optimization	
Glazing Type	General Clear 3 mm Glass
Total Solar Transmission (SHGC)	0,861
Light Transmission	0,898
Direct Solar Transmission	0,837
U-Value (ISSO 15099/NFRC) (W/m2-K)	5,894

Table A.8 – External windows of the optimized models

External Windows Post-Optimization	
Glazing Type	Vertical glazing, 0%-40% of wall, U-0.35 (1.99), SHGC-0.45
Total Solar Transmission (SHGC)	0,450
Light Transmission	0,560
Direct Solar Transmission	-
U-Value (ISSO 15099/NFRC) (W/m2-K)	1,990

Table A.9 – Internal windows of the optimized models

Internal Windows Post-Optimization	
Glazing Type	Vertical glazing, 0%-40% of wall, U-0.35 (1.99), SHGC-0.45
Total Solar Transmission (SHGC)	0,450
Light Transmission	0,560
Direct Solar Transmission	-
U-Value (ISSO 15099/NFRC) (W/m2-K)	1,990

Appendix III – Optimization graphical outputs

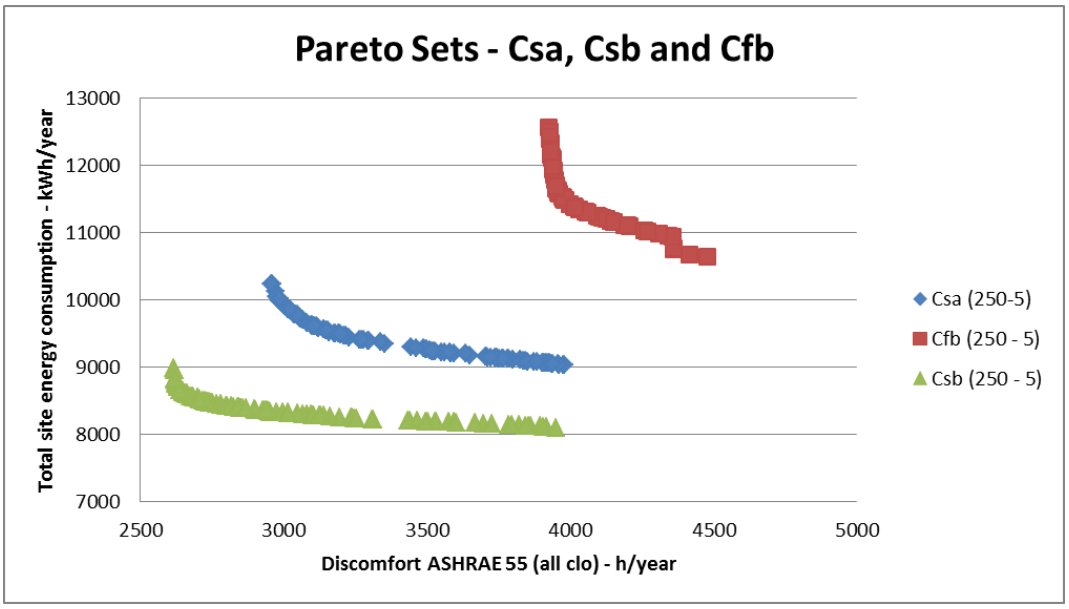

Figure A.4 – Graphical output for the Csa, Csb and Cfb climate zones

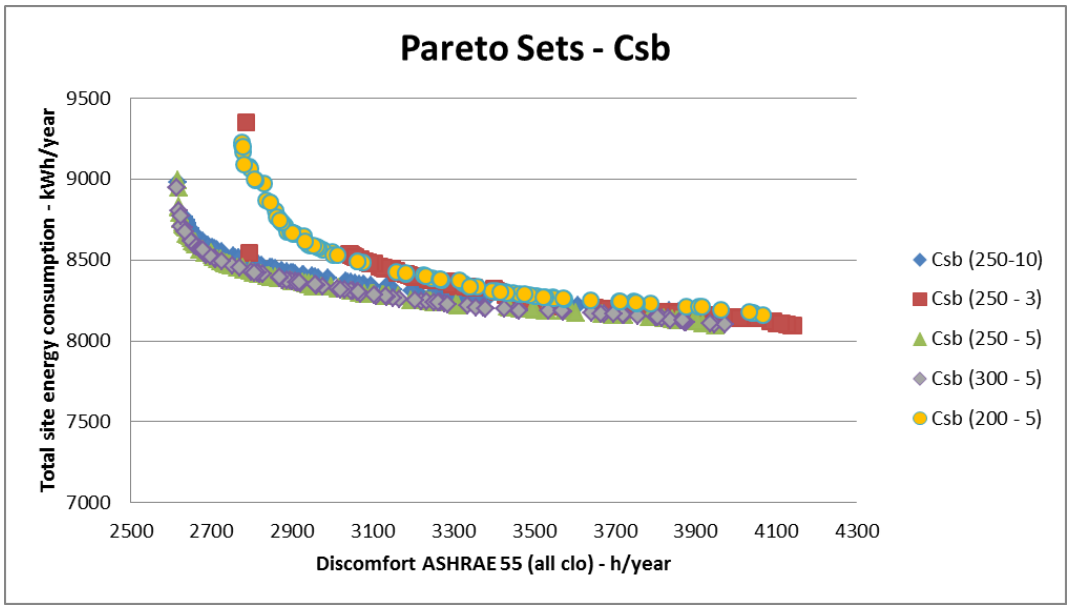

Figure A.5 – Graphical output for all the simulations corresponding to the Csb climate

Appendix IV – Performance results

Table A.10 – Results for the objective functions (Pareto 3, 4, 5, 6, 7, 8, 9 and 10)

Post-Optimization results: Appendix								
Optimized Features	Pareto 3	Pareto 4	Pareto 5	Pareto 6	Pareto 7	Pareto 8	Pareto 9	Pareto 10
Simulation	2	2	3	3	4	4	5	5
Climate	Csb	Csb	Csb	Csb	Csb	Csb	Csb	Csb
Number of generations	250	250	250	250	300	300	200	200
Population size	10	10	3	3	5	5	5	5
Minimization goal	Site Energy	Discomfort	Site Energy	Discomfort	Site Energy	Discomfort	Site Energy	Discomfort
Total site energy (kWh)	8127,08	8426,74	8117,55	8575,14	8114,66	8516,54	8141,7	8396,34
Discomfort ASHRAE 55 (all clo) (h)	3976	2615	3963	2644	3975	2617	3950	2618

Table A.11 – Results for the design variables (Pareto 3)

Pareto 3	
Simulation	2
Climate	Csb
Glazing type	Vertical glazing, 0%-40% of wall, U-0.35 (1.99), SHGC-0.45
Infiltration (ac/h)	0,000
Insulation - External wall construction	LSF with 216 mm insulation thickness
Insulation - Flat roof construction	Roof with 180 mm insulation thickness
Building orientation (º)	69,14

Table A.12 – Results for the design variables (Pareto 4)

Pareto 4	
Simulation	2
Climate	Csb
Glazing type	Vertical glazing, 0%-40% of wall, U-0.35 (1.99), SHGC-0.45
Infiltration (ac/h)	0,216
Insulation - External wall construction	LSF with 216 mm insulation thickness
Insulation - Flat roof construction	Roof with 180 mm insulation thickness
Building orientation (º)	57,67

Table A.13 – Results for the design variables (Pareto 5)

Pareto 5	
Simulation	3
Climate	Csb
Glazing type	Vertical glazing, 0%-40% of wall, U-0.35 (1.99), SHGC-0.45
Infiltration (ac/h)	0,000
Insulation - External wall construction	LSF with 216 mm insulation thickness
Insulation - Flat roof construction	Roof with 180 mm insulation thickness
Building orientation (º)	61,04

Table A.14 – Results for the design variables (Pareto 6)

Pareto 6	
Simulation	3
Climate	Csb
Glazing type	Vertical glazing, 0%-40% of wall, U-0.35 (1.99), SHGC-0.45
Infiltration (ac/h)	0,216
Insulation - External wall construction	LSF with 216 mm insulation thickness
Insulation - Flat roof construction	Roof with 180 mm insulation thickness
Building orientation (º)	62,73

Table A.15 – Results for the design variables (Pareto 7)

Pareto 7	
Simulation	4
Climate	Csb
Glazing type	Vertical glazing, 0%-40% of wall, U-0.35 (1.99), SHGC-0.45
Infiltration (ac/h)	0,000
Insulation - External wall construction	LSF with 216 mm insulation thickness
Insulation - Flat roof construction	Roof with 180 mm insulation thickness
Building orientation (º)	68,12

Table A.16 – Results for the design variables (Pareto 8)

Pareto 8	
Simulation	4
Climate	Csb
Glazing type	Vertical glazing, 0%-40% of wall, U-0.35 (1.99), SHGC-0.45
Infiltration (ac/h)	0,223
Insulation - External wall construction	LSF with 216 mm insulation thickness
Insulation - Flat roof construction	Roof with 180 mm insulation thickness
Building orientation (º)	45,87

Table A.17 – Results for the design variables (Pareto 9)

Pareto 9	
Simulation	5
Climate	Csb
Glazing type	Vertical glazing, 0%-40% of wall, U-0.35 (1.99), SHGC-0.45
Infiltration (ac/h)	0,000
Insulation - External wall construction	LSF with 216 mm insulation thickness
Insulation - Flat roof construction	Roof with 180 mm insulation thickness
Building orientation (º)	56,99

Table A.18 – Results for the design variables (Pareto 10)

Pareto 10	
Simulation	5
Climate	Csb
Glazing type	Vertical glazing, 0%-40% of wall, U-0.35 (1.99), SHGC-0.45
Infiltration (ac/h)	0,198
Insulation - External wall construction	LSF with 216 mm insulation thickness
Insulation - Flat roof construction	Roof with 180 mm insulation thickness
Building orientation (º)	56,66

Table A.19 – Performance results: Absolute values (Csb climate)

Performance parameters	Csb Climate										
	Pre-Optimization	Post-Optimization									
	Initial solution	E (250-5)	D (250-5)	E(250-10)	D(250-10)	E(250-3)	D(250-3)	E(300-5)	D(300-5)	E(200-5)	D(200-5)
	Model 1	Pareto 1	Pareto 2	Pareto 3	Pareto 4	Pareto 5	Pareto 6	Pareto 7	Pareto 8	Pareto 9	Pareto 10
Annual Total site energy (kWh/year)	14330,31	8115,40	8453,24	8127,08	8426,74	8117,55	8575,14	8114,66	8416,54	8141,70	8396,34
Annual Fuel totals (kWh/year)	9639,63	5134,49	5704,24	5133,47	5660,05	5131,82	5870,70	5130,67	5673,56	5142,01	5611,02
Annual operational CO2 emissions (kg/year)	5841,61	3111,50	3456,77	3110,88	3429,99	3109,88	3557,64	3109,18	3438,17	3116,05	3400,28
CDH - All Summer (h/year)	857	1366	823	1364	847	1360	823	1364	838	1359	871
HDH - All Winter (h/year)	2234	2578	1791	2605	1769	2594	1791	2604	1776	2583	1745
OT average- All Summer (°C)	23,95	24,74	24,46	24,77	24,49	24,76	24,46	24,77	24,47	24,75	24,50
OT average- All Winter (°C)	19,68	20,92	20,45	20,97	20,49	20,97	20,45	20,97	20,45	20,95	20,52
Discomfort ASHRAE 55 (all clo) (h)	3092	3948	2616	3976	2615	3963	2644	3975	2617	3950	2618

Table A.20 – Performance results: Absolute values (Csa climate)

Performance parameters	Csa Climate		
	Pre-Optimization	Post-Optimization	
	Initial solution	E (250-5)	D (250-5)
	Model 2	Pareto 11	Pareto 12
Annual Total site energy (kWh/year)	17168,79	9046,77	9865,32
Annual Fuel totals (kWh/year)	11701,72	5986,10	6792,88
Annual operational CO2 emissions (kg/year)	7091,24	3627,57	4116,48
CDH - All Summer (h/year)	972	1309	898
HDH - All Winter (h/year)	2311	2682	2063
OT average- All Summer (°C)	24,02	24,72	24,46
OT average- All Winter (°C)	19,49	20,57	20,20
Discomfort ASHRAE 55 (all clo) (h)	3279	3983	2955

Table A.21 – Performance results: Absolute values (Cfb climate)

Performance parameters	Cfb Climate		
	Pre-Optimization	Post-Optimization	
	Initial solution	E (250-5)	D (250-5)
	Model 3	Pareto 13	Pareto 14
Annual Total site energy (kWh/year)	24353,88	10680,75	11467,48
Annual Fuel totals (kWh/year)	22718,70	9849,08	10789,89
Annual operational CO2 emissions (kg/year)	13767,52	5968,53	6538,61
CDH - All Summer (h/year)	1045	2055	1036
HDH - All Winter (h/year)	3135	2692	3056
OT average- All Summer (°C)	21,93	22,88	22,64
OT average- All Winter (°C)	18,24	19,34	19,25
Discomfort ASHRAE 55 (all clo) (h)	4179	4751	4092

***** In some cases, the sum of CDH with HDH may not ensure the exact same result as the total of Discomfort hours as expected, due to rounding adjustements.

Table A.22 – Performance results: Relative values (Csb climate)

Performance parameters	Csb Climate										
	Pre-Optimization	Post-Optimization									
	Initial solution	Δ 1	Δ 2	Δ 3	Δ 4	Δ 5	Δ 6	Δ 7	Δ 8	Δ 9	Δ 10
	Model 1	Pareto 1	Pareto 2	Pareto 3	Pareto 4	Pareto 5	Pareto 6	Pareto 7	Pareto 8	Pareto 9	Pareto 10
Annual Total site energy (kWh/year)	-	-43,37%	-41,01%	-43,29%	-41,20%	-43,35%	-40,16%	-43,37%	-41,27%	-43,19%	-41,41%
Annual Fuel totals (kWh/year)	-	-46,74%	-40,83%	-46,75%	-41,28%	-46,76%	-39,10%	-46,78%	-41,14%	-46,66%	-41,79%
Annual operational CO2 emissions (kg/year)	-	-46,74%	-40,83%	-46,75%	-41,28%	-46,76%	-39,10%	-46,78%	-41,14%	-46,66%	-41,79%
CDH - All Summer (h/year)	-	59,48%	-3,92%	59,21%	-1,12%	58,78%	-3,92%	59,26%	-2,11%	58,70%	1,68%
HDH - All Winter (h/year)	-	15,42%	-19,84%	16,61%	-20,81%	16,13%	-19,84%	16,56%	-20,50%	15,63%	-21,87%
OT average- All Summer (°C)	-	3,33%	2,15%	3,42%	2,26%	3,38%	2,15%	3,43%	2,20%	3,36%	2,33%
OT average- All Winter (°C)	-	6,33%	3,93%	6,57%	4,10%	6,57%	3,93%	6,55%	3,92%	6,47%	4,27%
Discomfort ASHRAE 55 (all clo) (h)	-	27,68%	-15,39%	28,59%	-15,43%	28,17%	-14,49%	28,56%	-15,36%	27,75%	-15,33%

Table A.23 – Performance results: Relative values (Csa climate)

Performance parameters	Csa Climate		
	Pre-Optimization	Post-Optimization	
	Initial solution	Δ 11	Δ 12
	Model 2	Pareto 11	Pareto 12
Annual Total site energy (kWh/year)	-	-47,31%	-42,54%
Annual Fuel totals (kWh/year)	-	-48,84%	-41,95%
Annual operational CO2 emissions (kg/year)	-	-48,84%	-41,95%
CDH - All Summer (h/year)	-	34,70%	-7,62%
HDH - All Winter (h/year)	-	16,05%	-10,73%
OT average- All Summer (°C)	-	2,93%	1,85%
OT average- All Winter (°C)	-	5,55%	3,66%
Discomfort ASHRAE 55 (all clo) (h)	-	21,47%	-9,88%

Table A.24 – Performance results: Relative values (Cfb climate)

Performance parameters	Cfb Climate		
	Pre-Optimization	Post-Optimization	
	Initial solution	Δ 13	Δ 14
	Model 3	Pareto 13	Pareto 14
Annual Total site energy (kWh/year)	-	-56,14%	-52,91%
Annual Fuel totals (kWh/year)	-	-56,65%	-52,51%
Annual operational CO2 emissions (kg/year)	-	-56,65%	-52,51%
CDH - All Summer (h/year)	-	96,69%	-0,88%
HDH - All Winter (h/year)	-	-14,12%	-2,53%
OT average- All Summer (°C)	-	4,33%	3,24%
OT average- All Winter (°C)	-	6,03%	5,54%
Discomfort ASHRAE 55 (all clo) (h)	-	13,69%	-2,08%

Appendix V – Statistical analysis results

Table A.25 – Optimal design distribution (Simulations 2 and 3)

Optimal design distribution - Appendix (Part 1)				
Generation	Csb			
	Simulation 2 (250 - 10)	Distribution 2	Simulation 3 (250 - 3)	Distribution 3
0-50	18	16,98%	1	1,16%
51-100	24	22,64%	13	15,12%
101-150	18	16,98%	13	15,12%
151-200	22	20,75%	33	38,37%
201-250	24	22,64%	26	30,23%
251 - 300	-	-	-	-
Total	106	100,00%	86	100,00%

Table A.26 – Optimal design distribution (Simulations 4 and 5)

Optimal design distribution - Appendix (Part 2)				
Generation	Csb			
	Simulation 4 (300 - 5)	Distribution 4	Simulation 5 (200 - 5)	Distribution 5
0-50	0	0,00%	5	5,56%
51-100	12	15,00%	27	30,00%
101-150	13	16,25%	29	32,22%
151-200	19	23,75%	29	32,22%
201-250	19	23,75%	-	-
251 - 300	37	46,25%	-	-
Total	80	100,00%	90	100,00%

Table A.27 – Type solution configuration for the Csb climate (Simulation 5)

Type Solution - Csb climate			
Design Variables	Simulation 1 Design Settings	Number of options	Percentage
Glazing Type	Vertical glazing, 0%-40% of wall, U-0.35 (1.99), SHGC-0.45	107	100,00%
Infiltration (ac/h)	I < 0,05	30	28,04%
	0,05 ≤ I < 0,10	36	33,64%
	0,10 ≤ I < 0,15	24	22,43%
	0,15 ≤ I < 0,20	15	14,02%
	I > 0,20	2	1,87%
	Total	107	100,00%
Insulation - External wall construction	LSF with 216 mm insulation thickness	107	100,00%
Insulation - Flat roof construction	Roof with 180 mm insulation thickness	107	100,00%
Building orientation (°)	BO < 15	0	0,00%
	15 ≤ BO < 20	0	0,00%
	20 ≤ BO < 25	0	0,00%
	25 ≤ BO < 30	0	0,00%
	30 ≤ BO < 35	0	0,00%
	35 ≤ BO < 40	1	0,93%
	40 ≤ BO < 45	17	15,89%
	45 ≤ BO < 50	11	10,28%
	50 ≤ BO < 55	15	14,02%
	55 ≤ BO < 60	29	27,10%
	60 ≤ BO < 65	29	27,10%
	65 ≤ BO < 70	4	3,74%
	BO > 70	1	0,93%
	Total	107	100,00%

Table A.28 – Type solution configuration for the Csa climate (Simulation 6)

Type Solution - Csa climate			
Design Variables	Simulation 6 Design Settings	Number of options	Percentage
Glazing Type	Vertical glazing, 0%-40% of wall, U-0.35 (1.99), SHGC-0.45	108	0,00%
Infiltration (ac/h)	I < 0,05	49	45,37%
	0,05 ≤ I < 0,10	22	20,37%
	0,10 ≤ I < 0,15	23	21,30%
	0,15 ≤ I < 0,20	12	11,11%
	I > 0,20	2	1,85%
	Total	108	100,00%
Insulation - External wall construction	LSF with 216 mm insulation thickness	108	100,00%
Insulation - Flat roof construction	Roof with 180 mm insulation thickness	108	100,00%
Building orientation (°)	BO < 15	1	0,93%
	15 ≤ BO < 20	1	0,93%
	20 ≤ BO < 25	7	6,48%
	25 ≤ BO < 30	11	10,19%
	30 ≤ BO < 35	21	19,44%
	35 ≤ BO < 40	25	23,15%
	40 ≤ BO < 45	12	11,11%
	45 ≤ BO < 50	28	25,93%
	50 ≤ BO < 55	2	1,85%
	55 ≤ BO < 60	0	0,00%
	60 ≤ BO < 65	0	0,00%
	65 ≤ BO < 70	0	0,00%
	BO > 70	0	0,00%
	Total	108	100,00%

Table A.29 – Type solution configuration for the Cfb climate (Simulation 7)

Type Solution - Cfb climate			
Design Variables	Simulation 7 Design Settings	Number of options	Percentage
Glazing Type	Vertical glazing, 0%-40% of wall, U-0.35 (1.99), SHGC-0.45	62	100,00%
Infiltration (ac/h)	I < 0,05	9	14,52%
	0,05 ≤ I < 0,10	16	25,81%
	0,10 ≤ I < 0,15	28	45,16%
	0,15 ≤ I < 0,20	9	14,52%
	I > 0,20	0	0,00%
	Total	62	100,00%
Insulation - External wall construction	LSF with 216 mm insulation thickness	62	100,00%
Insulation - Flat roof construction	Roof with 180 mm insulation thickness	62	100,00%
Thermal mass construction	Wooden window frame	6	9,68%
	Dummie (U=glass; other props=PVCframe)	3	4,84%
	Aluminium window frame (with thermal break)	47	75,81%
	UPVC window frame	6	9,68%
	Total	62	100,00%